

AD-A103 270

ABERDEEN UNIV (SCOTLAND) DEPT OF ENGINEERING
APPLICATION OF NUMERICAL METHODS TO THE CALCULATION OF ELECTRO--ETC(U)
AUG 81 J R SMITH, P LEES, D MCALLISTER AFOSR-80-0223

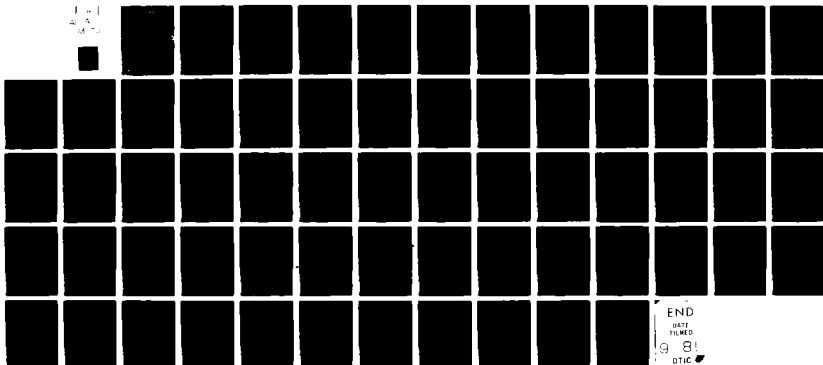
EOARD-TR-81-9

F/6 1/3

NL

UNCLASSIFIED

REF ID:
A221
M70



END
DATE
FILED
9 81
OTIC

AD A103270

BOARD 1161.9

LEVEL

(2)

Grant Number AFOSR-80-0223

APPLICATION OF NUMERICAL METHODS TO THE CALCULATION OF ELECTROSTATIC
FIELDS IN AIRCRAFT FUEL TANKS

J.R. Smith.
Department of Engineering,
University of Aberdeen.

P. Lees
Department of Engineering
University of Aberdeen.

D. McAllister
Dept. of Engineering
University of Aberdeen.

August 1981

Final Scientific Report, 1 July 1980 - 30 June 1981

Approved for public release; distribution unlimited.

Prepared for

EUROPEAN OFFICE OF AEROSPACE RESEARCH AND DEVELOPMENT,
London, England.

DTIC FILE COPY

455

413-411

81 821 013

REPORT DOCUMENTATION PAGE			READ INSTRUCTIONS BEFORE COMPLETING FORM
1. Report Number <i>AFOSR-80-0223</i>	2. Govt Accession No.	3. Recipient's Catalog Number	
4. Title (and Subtitle) Application of numerical methods to the calculation of electrostatic fields in aircraft fuel tanks.		5. Type of Report & Period Covered Scientific Report, 1 July 1980 — 30 June 1981,	
7. Author(s) <i>J.R. Smith, P. Lees D. McAllister</i>		6. Performing Org. Report Number <i>AFOSR-80-0223</i>	
9. Performing Organization Name and Address Department of Engineering, University of Aberdeen, Scotland		10. Program Element, Project, Task Area & Work Unit Numbers AFOSR AFWAL 61102F 62203F 2301/D1 3048/05	
11. Controlling Office Name and Address European Office of Aerospace Research and Development Box 14, FPO New York 09510		12. Report Date <i>11 August 1981</i>	
14. Monitoring Agency Name and Address European Office of Aerospace Research and Development Box 14, FPO New York 09510		15. <i>15 E 341 D</i>	
16. & 17. Distribution Statement Approved for public release; distribution unlimited.			
18. Supplementary Notes			
19. Key Words Electrostatic fields, finite element method, fuel tanks			
20. Abstract The solution of electrostatic field problems occurring during the refuelling of aircraft fuel tanks containing explosion suppressant foams is discussed. A computational model of a fuel tank is set up, and the finite element method is used to calculate the electrostatic potential distribution within the tank.			

Accession For NTIS GT&I DTIC T-8 Unannounced Justification	<input checked="" type="checkbox"/>
By _____	<input type="checkbox"/>
Distribution	<input type="checkbox"/>
Availability Codes A - All and/or S - Special	<input type="checkbox"/>
A	B

This report has been reviewed by the EOARD Information Office and is releasable to the National Technical Information Service (NTIS). At NTIS it will be releasable to the general public, including foreign nations.

This technical report has been reviewed and is approved for publication.

Owen Mancarella

OWEN MANCARELLA
Lt Colonel, USAF
Director, Aeronautical Systems

Gordon L. Hermann

GORDON L. HERMANN
Lt Colonel, USAF
Deputy Commander

1. ELECTROSTATIC HAZARDS IN AIRCRAFT FUEL TANKS DURING REFUELING

The generation of high levels of electrostatic charge in hydrocarbon fuels (such as JP-4) during aircraft refuelling has long been recognized as an explosion hazard. The fuel is pumped at high flow rates through pipes, hoses, and filter/separators, and hence is exposed to relatively large liquid/solid interfaces. The double layer created at these interfaces coupled with the movement of fuel across them leads to a net unipolar charge being acquired by the fuel as it is swept along. The high charging tendency of a fuel such as JP-4, coupled with a low conductivity (typically $< 10 \text{ pS/m}$) can lead to hazardous charge accumulation in the receiving tank. If resulting local electrostatic fields on the fuel surface exceed the breakdown value for the vapour space, electrostatic discharges may occur. Such a discharge may be incendive if (i) it has sufficient energy, and (ii) the fuel/air mixture lies in a flammable range (i.e. will support combustion). It is thus patently of importance to be able to estimate electrostatic potential and field distributions in fuel tanks for given charge distributions.

The introduction of polyurethane foam into fuel tanks to act as an explosion suppressant presents an additional problem. The foam itself acts as a secondary charge generating surface for the fuel (Ref. 1). The relaxation time of the charge in the tank increases enormously, thus leading to substantially increased levels of accumulated charge in the tank, since the charge is unable to relax to earth.

The present study is an attempt to apply numerical and computational techniques to the problem in order to examine the feasibility of providing useful working guides for estimating electrostatic potentials and fields in fuel tanks containing such foams.

2. THE MATHEMATICAL PROBLEM AND THE FINITE ELEMENT METHOD

One method of approach to the problem is to consider the fuel tank at various levels of filling, postulate a charge distribution and boundary conditions, and solve Poisson's equation for this situation. This approach has been tackled analytically for some very simple geometries and charge distributions (Refs. 2,3). For the modelling of realistic situations, however, the analysis becomes intractable, and recourse to numerical methods becomes essential.

Various numerical techniques for approximating the solution of electrostatic field problems are currently in use. These include the finite-difference method, the charge simulation method, the boundary integral method, and the finite element method. The method chosen for this study is the finite element method. It allows the modelling of complicated geometries, inhomogeneous charge distributions, and dielectric changes within the region of interest. Its disadvantages are relatively large data input and large computer storage requirements.

The basic mathematical problem to be tackled is the solution of Poisson's equation

$$\nabla^2\phi = -\frac{\rho}{\epsilon_0 \epsilon_r}$$

within a region, subject to certain boundary conditions. Here, ϕ is the electrostatic potential, ρ is the space charge density, ϵ_0 is the

absolute permittivity (8.854×10^{-12} F/m) and ϵ_r is the relative dielectric constant of the medium. To provide a complete definition of problem, one or more of the following boundary conditions are required:

(i) $\phi = f(s)$ which fixes the potential at the boundary s , as a specified function $f(s)$ of position.

(e.g. on an earthed boundary $\phi = 0$)

(ii) $\frac{\partial \phi}{\partial n} = 0$ which forces equipotentials to cross a boundary normally

(iii) $\frac{\partial \phi}{\partial n} = h(s)$ which superimposes a surface charge density distribution on a boundary.

Let us now consider the functional

$$F = \int_V \frac{1}{2} \{ |\nabla \phi|^2 - \frac{2\rho}{\epsilon_0 \epsilon_r} \phi \} dV + \int_S h \phi dS$$

where V is the volume of the region of interest contained by the bounding surface S . If we minimise this functional, i.e. look for admissible potential functions ϕ such that

$$\delta F = 0$$

it may be shown that the ensuing Euler-Lagrange equation is

$$\nabla^2 \phi = - \frac{\rho}{\epsilon_0 \epsilon_r}$$

i.e. the potential function must satisfy Poisson's equation, subject to appropriate boundary conditions.

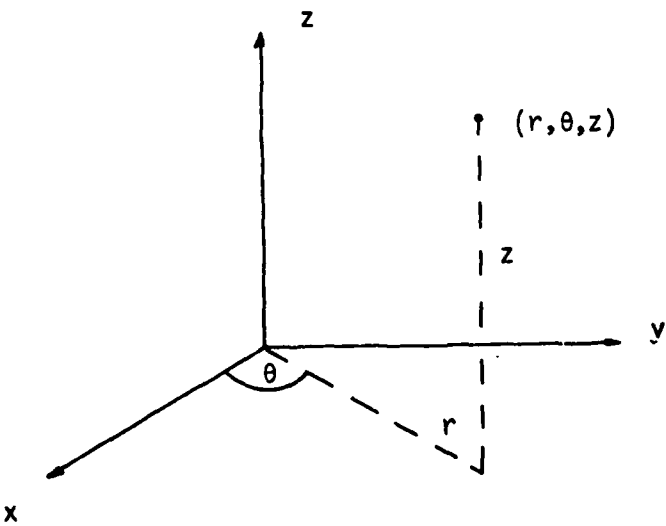
Briefly, the finite element method utilizes the above results by subdivision of the region of interest into a collection of elements, and approximating the potential by a set of piecewise continuous functions on these. Each element has a fixed number of nodes, and the

minimisation is performed in each element with respect to the potential values at these nodes.

For a full three-dimensional problem, however, the resulting set of linear equations in the nodal potentials to be solved is generally very large, and necessitates substantial computing resources. For many problems, however, including the one under consideration, the problem size may be reduced in size and complexity by using special features of the geometry. It will be seen that for the fuel tank under consideration, the geometry may be taken to be axisymmetric, yielding results which are sufficiently accurate to make the approximation acceptable. To exploit axisymmetry, cylindrical coordinates are adopted, and Poisson's equation becomes, in a usual notation,

$$\frac{1}{r} \frac{\partial}{\partial r} \left(r \frac{\partial \phi}{\partial r} \right) + \frac{1}{r^2} \frac{\partial^2 \phi}{\partial \theta^2} + \frac{\partial^2 \phi}{\partial z^2} = - \frac{\rho}{\epsilon_0 \epsilon_r} \quad (1)$$

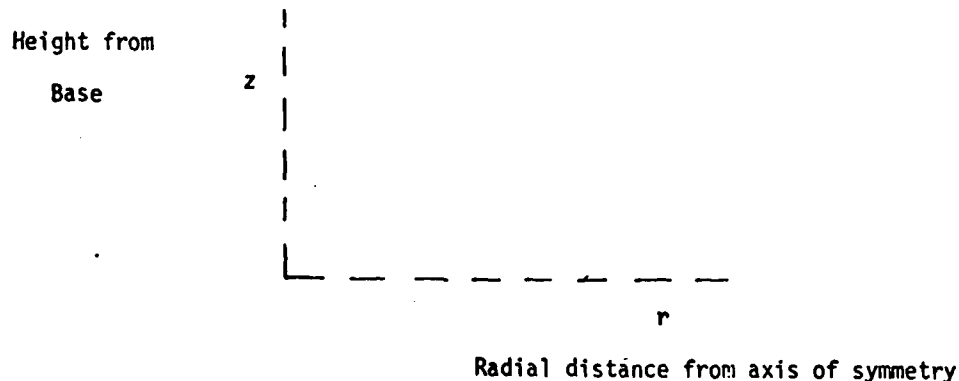
where r , θ , z are cylindrical coordinates as shown:



For axisymmetric problems, the geometry and charge distributions are rotationally symmetric, the potential ϕ , hence rotationally symmetric, and therefore independent of θ . Poisson's equation thus reduces to

$$\frac{1}{r} \frac{\partial}{\partial r} (r \frac{\partial \phi}{\partial r}) + \frac{\partial^2 \phi}{\partial z^2} = - \frac{\rho}{\epsilon_0 \epsilon_r} \quad (2)$$

The problem is thus basically two-dimensional:



The finite element method consists of four basic steps. Firstly a grid of numbered nodal points is established over the region of interest, including the boundary. At each interior node the value of potential is to be determined. On the boundary ϕ or $\frac{\partial \phi}{\partial n}$, its normal derivative, is given. Secondly the nodes are interconnected to form a finite number of subregions which collectively approximate the region of interest.

Thirdly the potential is approximated by a continuous function over each subregion, continuity conditions being imposed at subregion boundaries. Finally the unknown values of the potential at the node points are calculated by means of a variational principle, e.g. minimisation of electrostatic energy.

The subregions used in this case are triangular. A first order interpolating polynomial (3) is used to approximate the potential distribution over each triangle.

$$\phi = \alpha_1 + \alpha_2 r + \alpha_3 z \quad (3)$$

Thus in a triangle whose nodes are labelled i, j, k we have -

$$\phi_i = \alpha_1 + \alpha_2 r_i + \alpha_3 z_i$$

$$\phi_j = \alpha_1 + \alpha_2 r_j + \alpha_3 z_j$$

$$\phi_k = \alpha_1 + \alpha_2 r_k + \alpha_3 z_k$$

The variables α_1 , α_2 , α_3 can therefore be obtained in terms of ϕ_i , ϕ_j , ϕ_k and the coordinates of the nodes i, j, k. Substituting back into the interpolating polynomial (3) gives -

$$\phi = N_i \phi_i + N_j \phi_j + N_k \phi_k \quad (4)$$

where N_i , N_j , N_k are functions of r_i , r_j , r_k , z_i , z_j , z_k , r and z .

$\frac{\partial \phi}{\partial r}$ and $\frac{\partial \phi}{\partial z}$ may also be readily obtained.

The unknown values of α_1 , α_2 , α_3 may now be obtained by minimising the functional -

$$F = \int_A \left\{ r \left(\frac{\partial \phi}{\partial r} \right)^2 + r \left(\frac{\partial \phi}{\partial z} \right)^2 - \frac{2\rho r \phi}{\epsilon_o \epsilon_r} \right\} dA - 2 \int_C \phi h(s) ds$$

i.e. $\delta F = 0$

It is not difficult to show that this minimisation is equivalent to the requirement that ϕ satisfies the axisymmetric Poisson equation with appropriate boundary conditions.

Substitution of the appropriate local expressions for ϕ , $\frac{\partial \phi}{\partial r}$ and $\frac{\partial \phi}{\partial z}$ into the functional, and minimisation by a Rayleigh-Ritz or equivalent technique yields a set of simultaneous equations in the nodal potentials for each triangle. These elemental equations are then assembled to give a global set of equations which may be solved using standard techniques.

3. DESCRIPTION OF COMPUTATIONAL MODEL

(i) Geometry

The computational model used is based on the drawings of an A-10 fuel tank (Ref. 4). The real tank configuration (Figure 1) is such as to permit an axisymmetric approximation. The axisymmetric configuration chosen is shown in Figure (2), cut away to show the inlet nozzle and the explosion suppressant foam blocks. A dimensional cross-section of the tank is shown in Figure (3). (Dimensions are in millimetres).

(ii) Boundary Conditions

Figure (4) illustrates the assumed boundary conditions. The tank walls and the inlet nozzle are assumed to be at earth potential ($\phi = 0$).

Conforming to the real situation, the foam is divided into two categories, fixed and removable. Section 4 in Figure (4) corresponds to the fixed foam region. Sections 1,2, and 3 correspond to removable foam target sections. Thus, possible target configurations are Section 1 only, Sections 1 and 2 together, or Sections 1,2, and 3 together, allowing alteration of the voiding volume.

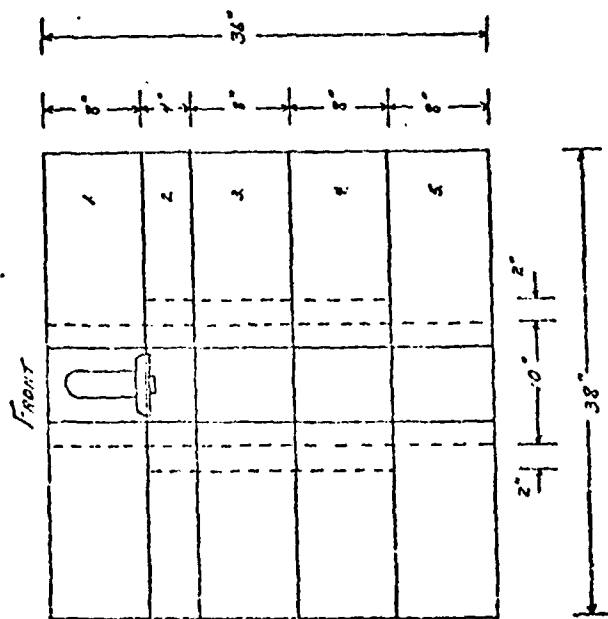
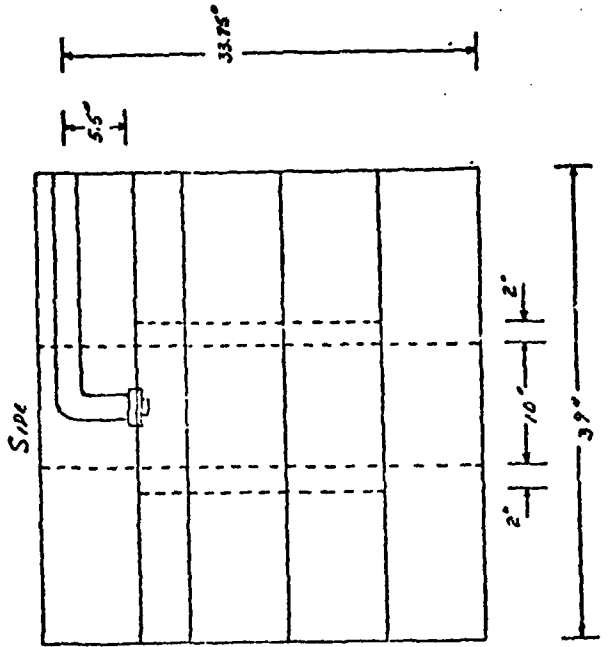
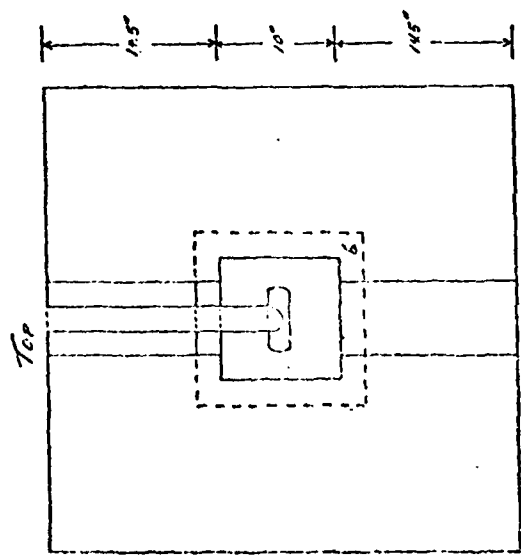
The dielectric boundaries of the foam blocks are also shown in Figure (4), as is the axis of symmetry. Since the problem is axisymmetric, the potential ϕ must satisfy $\frac{\partial \phi}{\partial n} = n$ on the axis of symmetry, i.e. the equipotentials must cross the axis normally.

(iii) The Charge Density

Accurate estimations of the volume and surface charge densities occurring when fuel is pumped at speed into a receiving tank are difficult

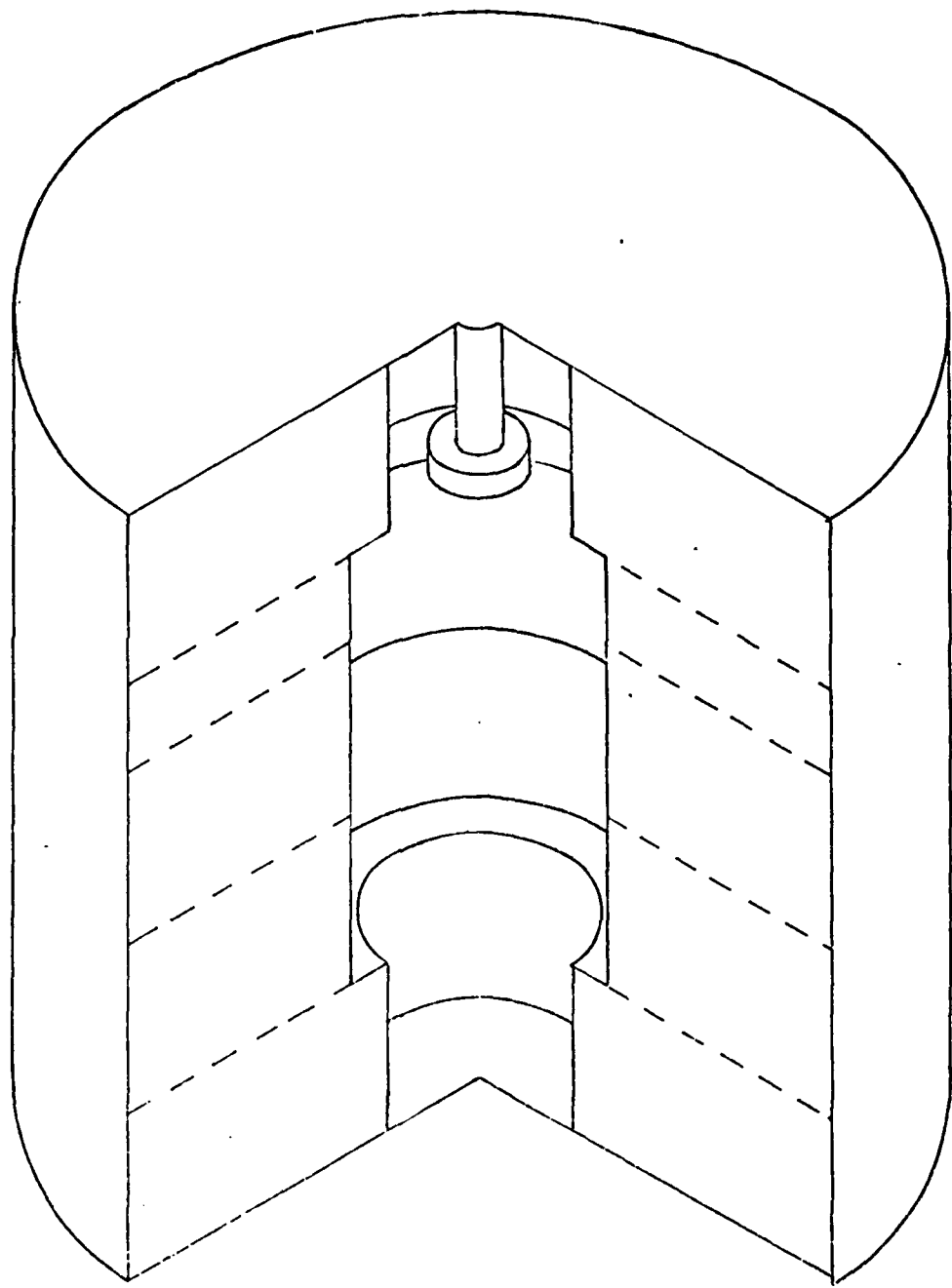
VOLUME CONCERN ILLUSTRATES FUTURE POSITION
 BLUE CONCERN PAPER FROM CENTER
 FOR THE F-4 AIRCRAFT

1. TOP PIECE OF FRAME WITH A 10' 10" 8" VOID AND A 6' 3" X 6' 6" HOLLOW
2. REMOVABLE PIECE OF FRAME WITH A 10' 10" 8" VOID AND A 6' 3" X 6" HOLLOW
3. MIDDLE PIECE OF FRAME WITH A 10' 10" 8" VOID AND A 6' 1" X 6" HOLLOW
4. BOTTOM MIDDLE PIECE OF FRAME WITH A 10' 10" 8" VOID AND A 6' 1" X 6" HOLLOW
5. BOTTOM PIECE OF FRAME WITH A 10' 10" 8" VOID AND A 6' 1" X 6" HOLLOW
6. THREE FRAME SECTION 10' 10" X 20' WITH A 10' 10" X 20' VOID.



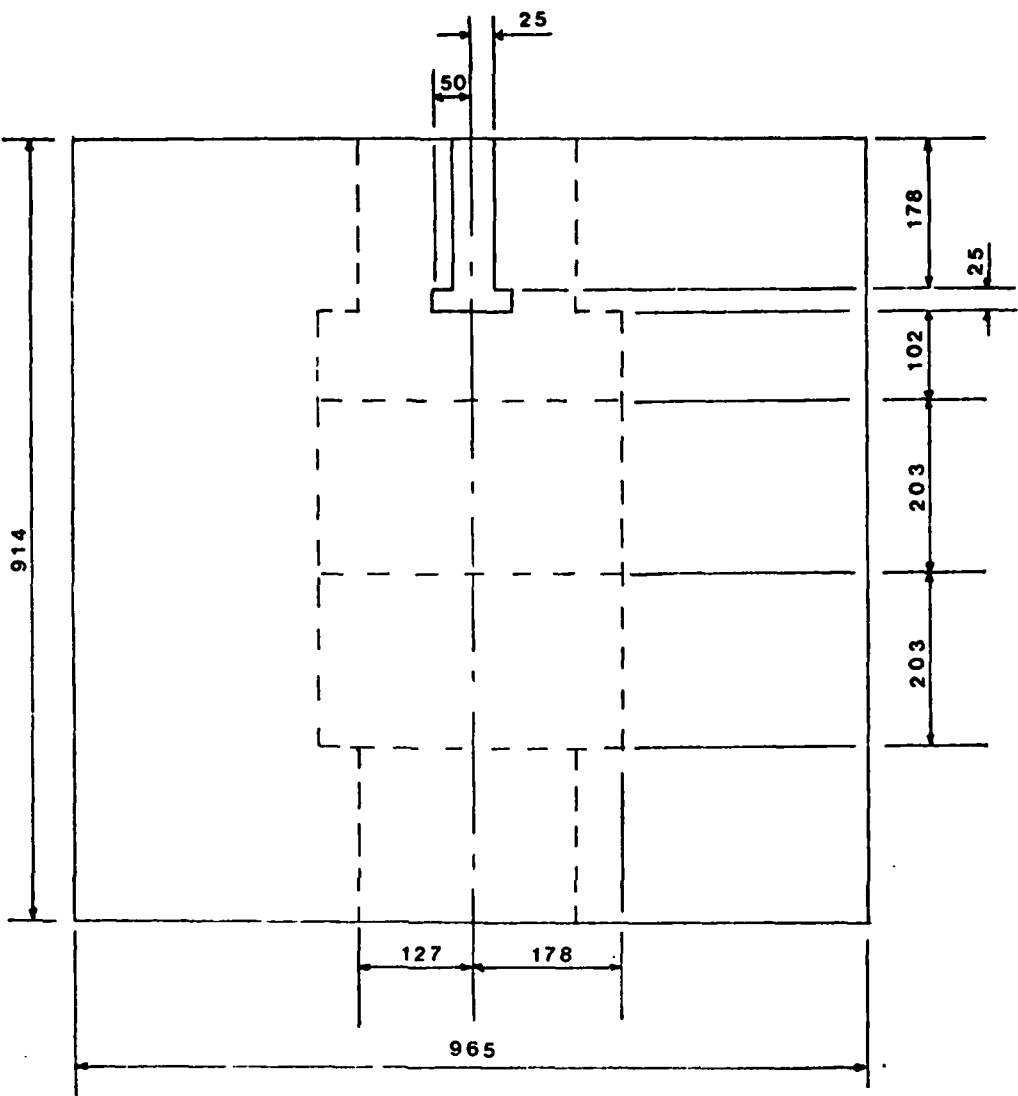
A-10 Fuel Tank

Fig. 1.



Isometric Projection of Tank Model

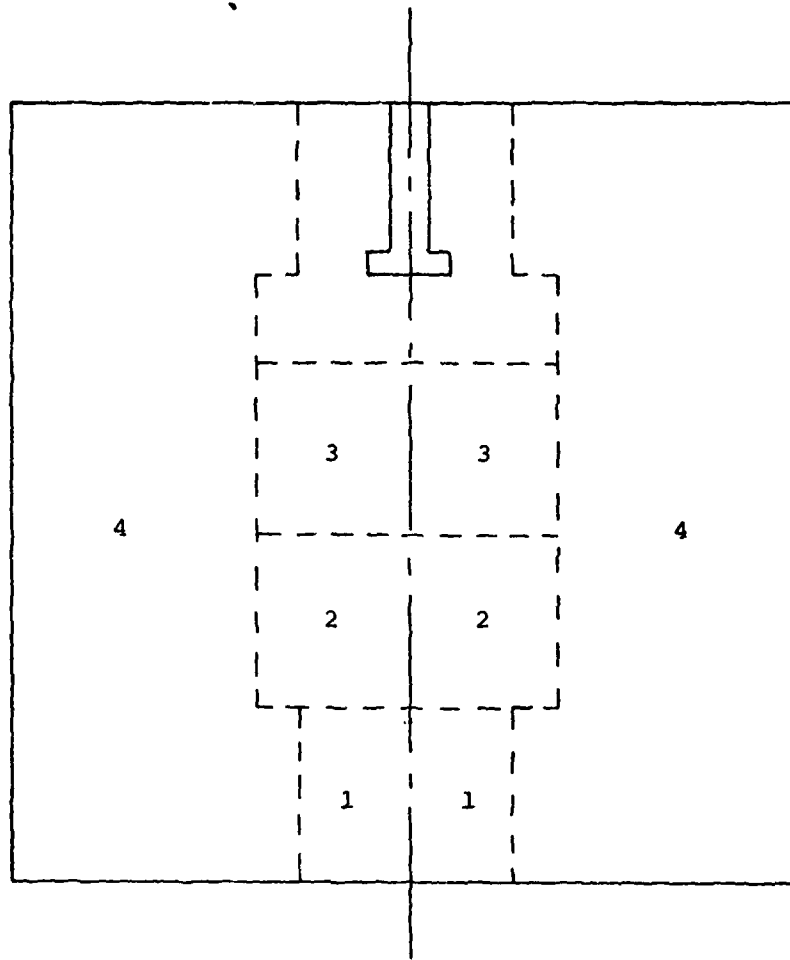
fig. 2.



All Dimensions in mm.

Dimensioned Section of Tank Model

fig. 3.



- Earthed boundaries
- - - Dielectric boundaries
- Axis of symmetry
- 1 Target section 1
- 2 Target section 2
- 3 Target section 3
- 4 Fixed foam region

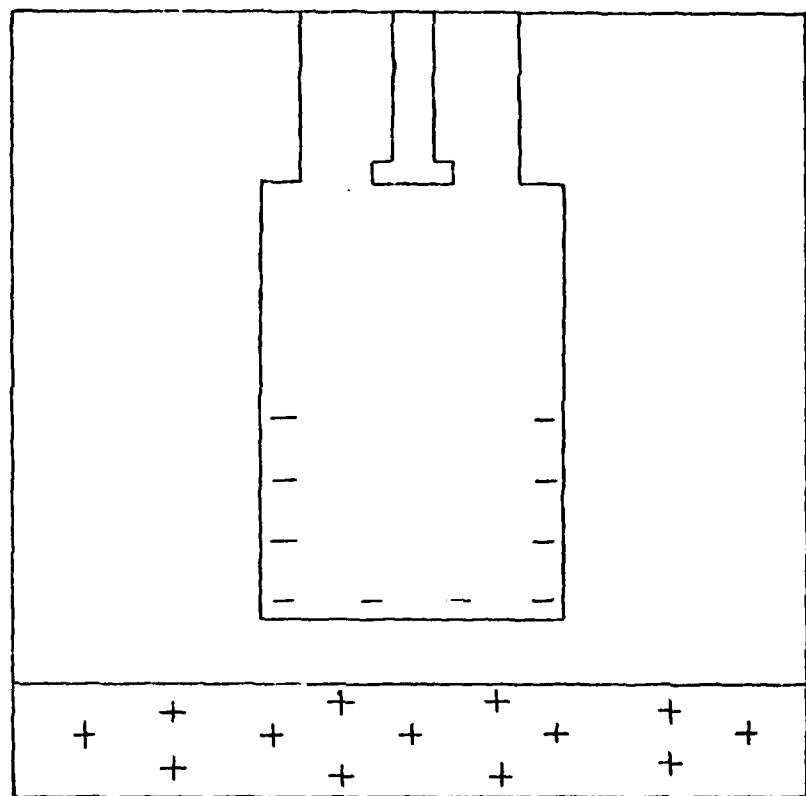
Section of Tank Model showing Target Sections

fig. 4.

to obtain. Factors such as fuel conductivity, rate of flow, turbulence, all contribute to the distribution of charge in the fuel at any particular time. The simplest, and not unrealistic, distribution to assume is a constant charge density within the fuel. There is evidence (Ref. 5) that jet fuels such as JP-4 generate static electricity when passing through porous media. The explosion suppressant foam acts as a secondary static charge generating surface. Furthermore, the movement of charge with foam present is very slow, so a constant charge density at any filling level is a reasonable approximation. The dielectric constant of both fuel and foam has been taken to be 2. A typical charge distribution considered is shown in Figure (5). As we shall see, the charge distributions studied at various filling levels allow a wide choice of postulated charge distribution.

4. RESULTS

The cases studied consist of charge distributions, both volume and surface, for various filling levels, and for different target sections. A 'standard' constant volume charge distribution of 10^{-4} C/m^3 in the fuel was chosen, together with a 'standard' surface charge distribution of 10^{-3} C/m^2 on the foam surface in the voiding region. This is not restricted since the two charge distributions are treated separately, and the principle of superposition allows simple scaling to a desired charge density. The plots provided give ten equipotentials between minimum and maximum potentials for each situation. Also given are plots of electrostatic field along the axis of symmetry for each configuration.



Typical Charge Distribution

Fig.5.

PLOTS 1 - 17

The configuration for plots 1-17 consists of foam Section 4 together with foam Section 1 inserted. (See Figure 6).

Plots 1 - 5 Charge density in fuel $\approx 10^{-4} \text{ C/m}^3$

Charge density on foam surface = 0 C/m^2

Filling levels at .1, .2, .3, .4, .5 metres above base.

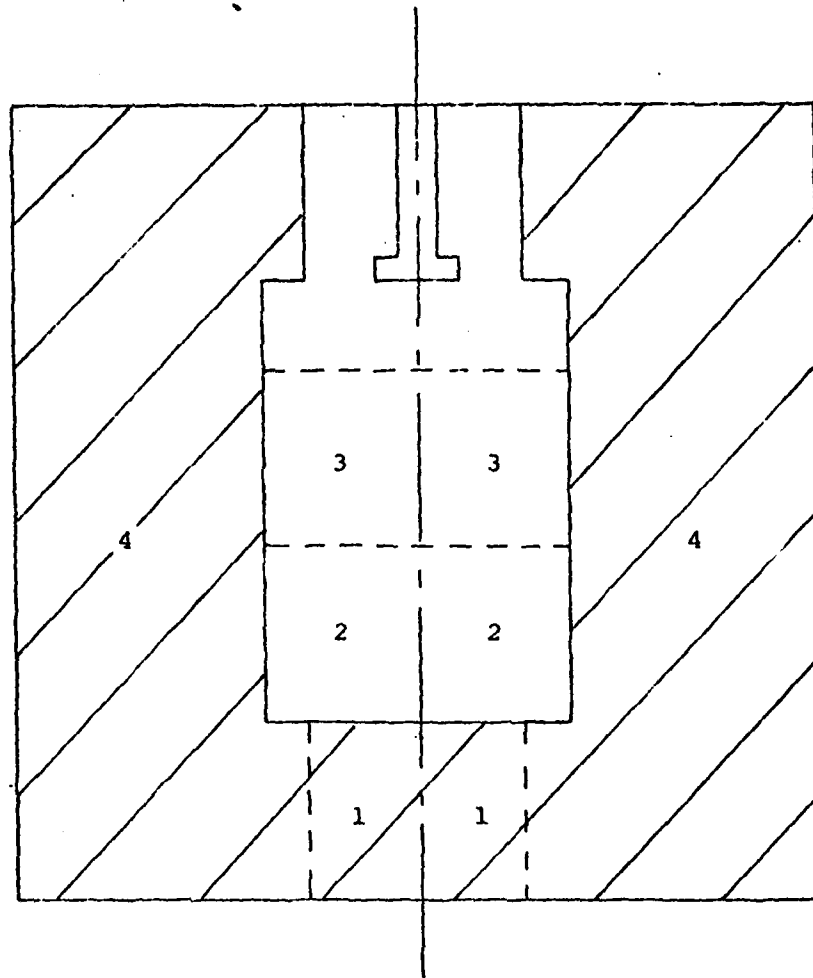
Plot 6 Surface charge density of 10^{-3} C/m^2 on Section 1

upper surface only.

Plots 7 - 11 Surface charge on Section 1 upper surface and at heights .1, .2, .3, .4, .5 metres above this surface.

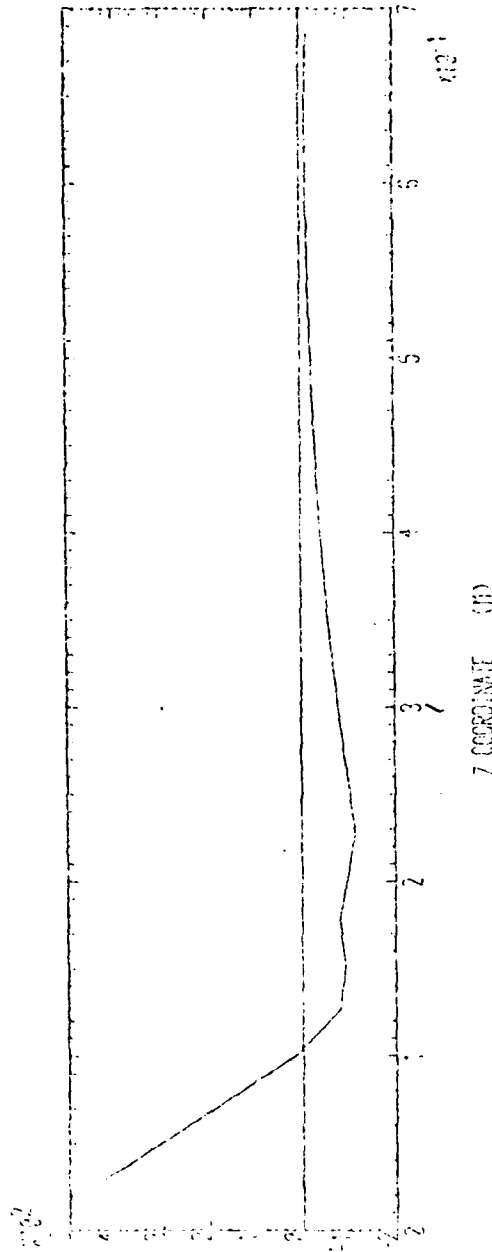
Plot 12 Vertical stream of fuel with charge density 10^{-4} C/m^3 impinging on the target area.

Plots 13 - 17 Vertical stream of fuel + voiding region filled to heights .1, .2, .3, .4, .5 metres.



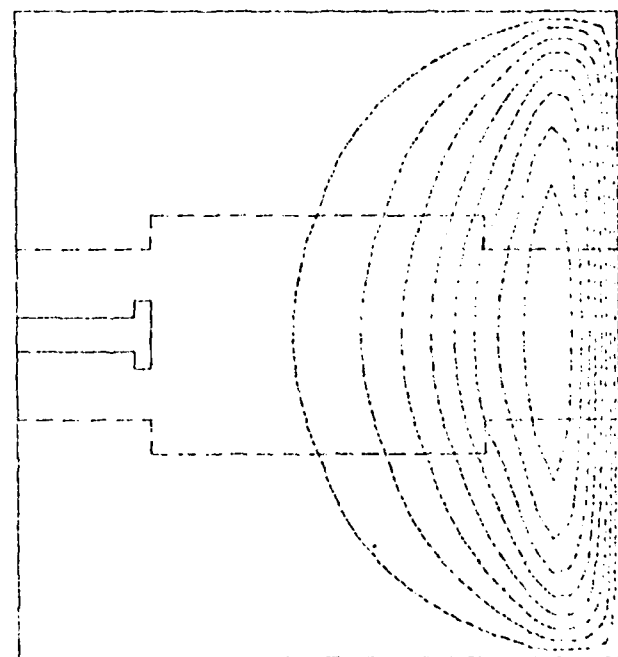
Foam sections 1 and 4 in place

fig. 6.

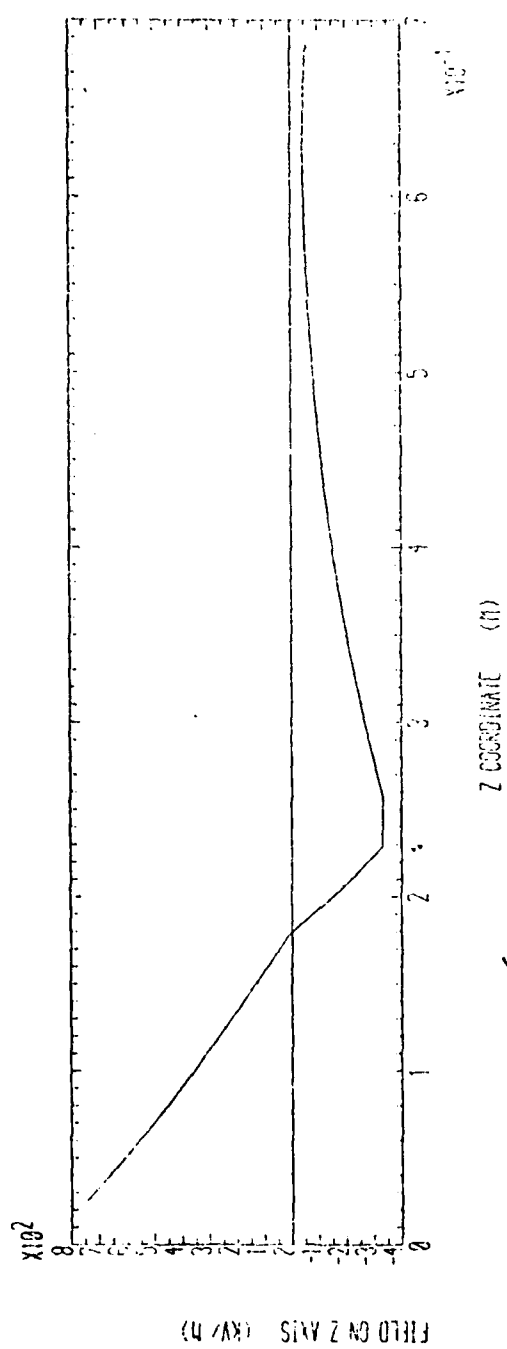


(a) 2D SIMULATION

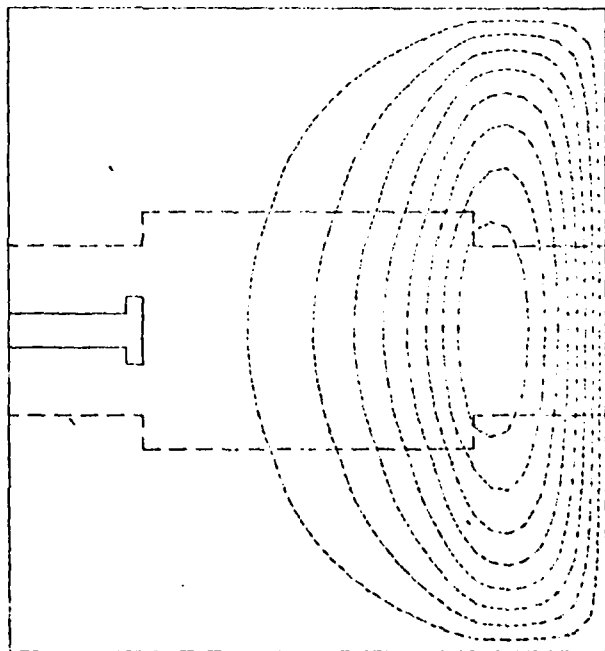
MINIMUM POTENTIAL	UV1 .2332E 0
MAXIMUM POTENTIAL	UV1 .3043E 5
CHARGE DENSITY IN FUEL	UV11 .1332E -3
CHARGE DISTRIBUTION ON FOAM	UV121 .3332E 0
FILLING LEVEL	UV1 .1016E 0
CONTOUR SPACING	UV1 .3333E 4



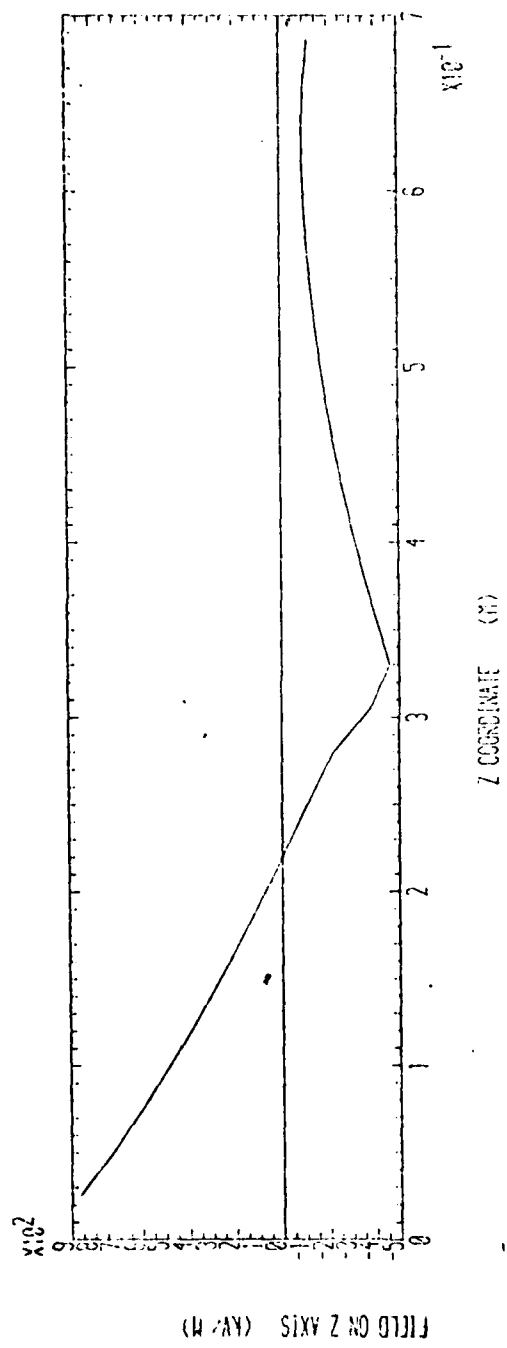
PLOT 1



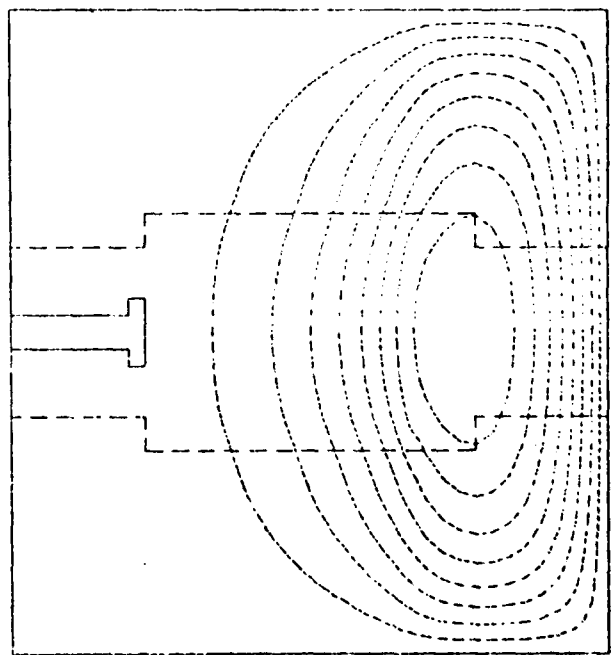
MINIMUM POTENTIAL	1KV	CONST.
MAXIMUM POTENTIAL	6KV	CONST.
CHARGE DENSITY IN FUEL	CONST.	CONST.
CHARGE DISTRIBUTION ON FUEL	CONST.	CONST.
FILLING LEVEL	1.2M	CONST.
CONTOUR SPACING	1.8M	CONST.



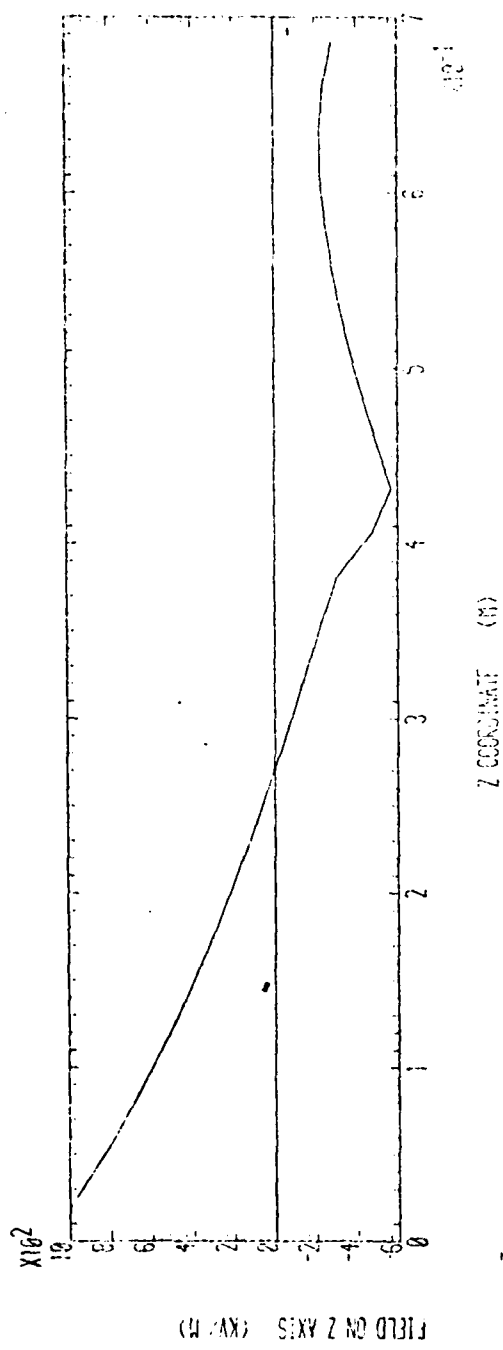
PLOT 2



MINIMUM POTENTIAL 0KV
 MAXIMUM POTENTIAL 6KV
 CHARGE DENSITY IN FUEL 0.0000E+0
 CHARGE DISTRIBUTION ON FOAM 0.0000E+0
 FILLING LEVEL 0.0000E+0
 CONTOUR SPACING 0.0000E+0

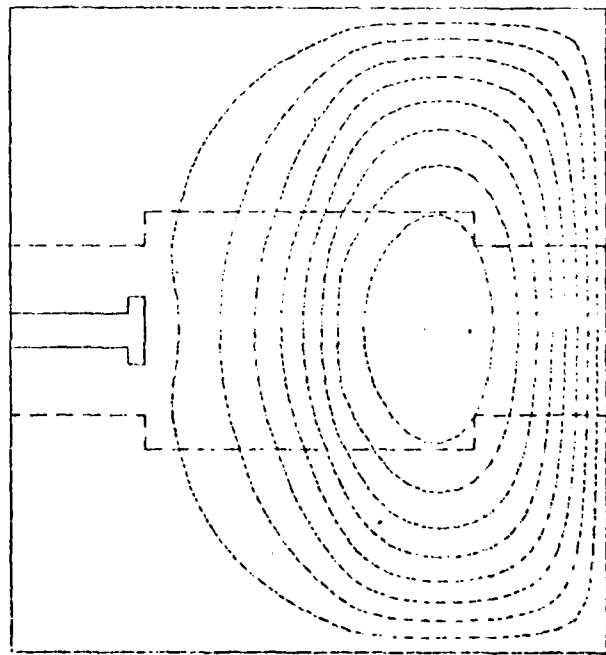


PLOT 3

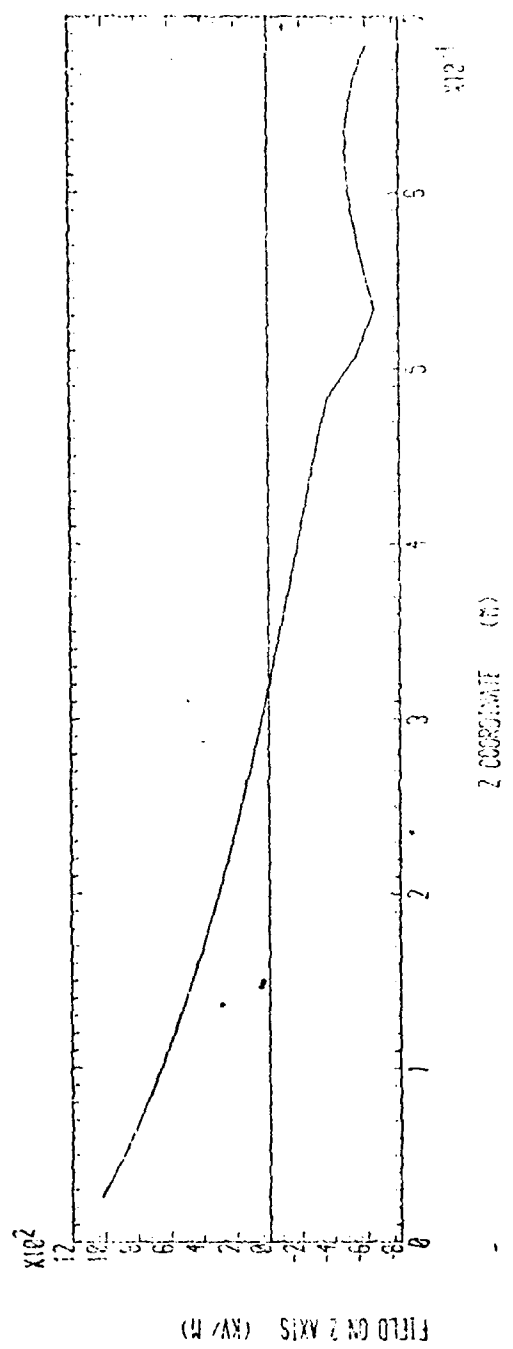


(MAX) SIX X NO 01313

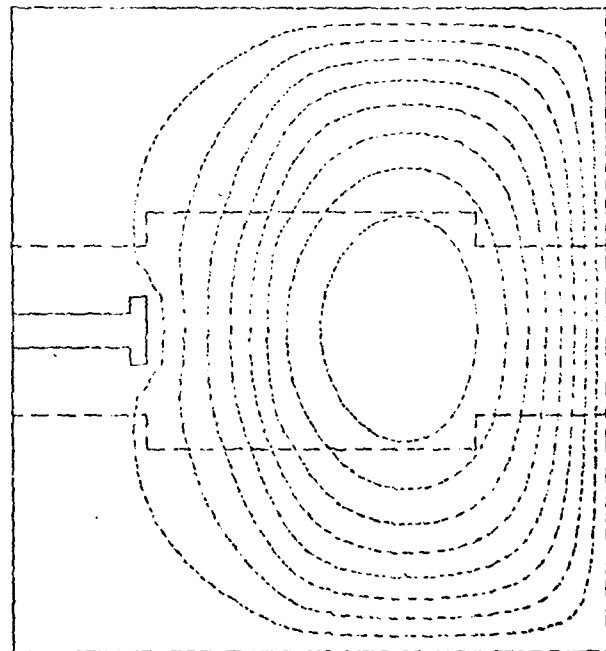
MINIMUM POTENTIAL	5 kV	CHARGE	2
MAXIMUM POTENTIAL	10 kV	CHARGE	3
CHARGE DENSITY IN FUEL	10.730	CHARGE	3
CHARGE DISTRIBUTION ON FOAM	10.7123	CHARGE	3
FILLING LEVEL	2.1	CHARGE	2
CONTOURS SPACING	5 kV	CHARGE	3



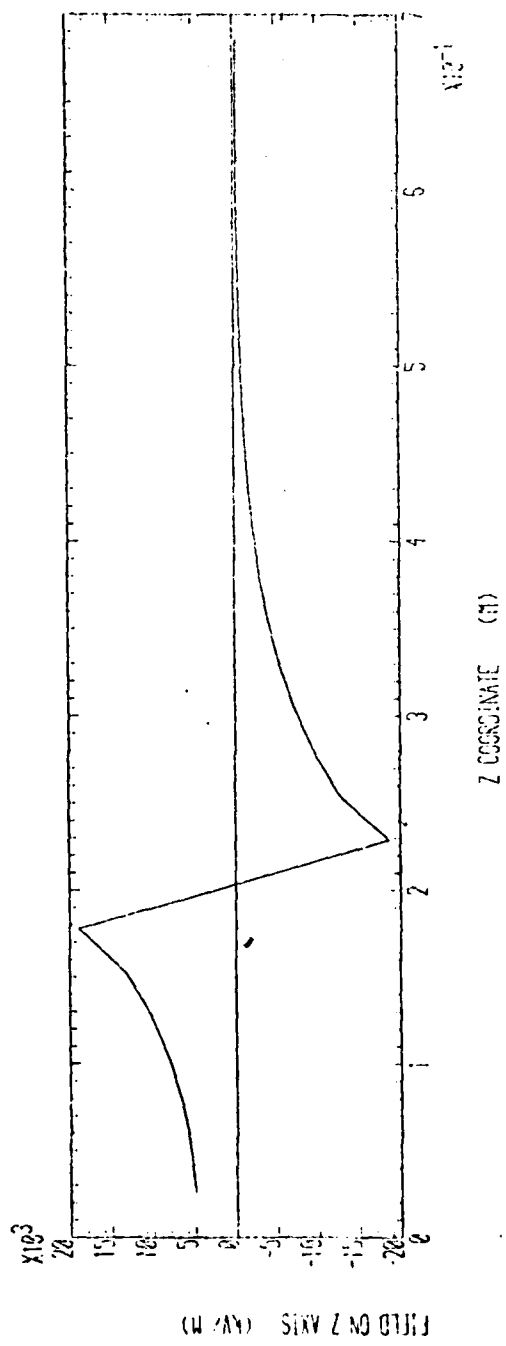
PLOT 4



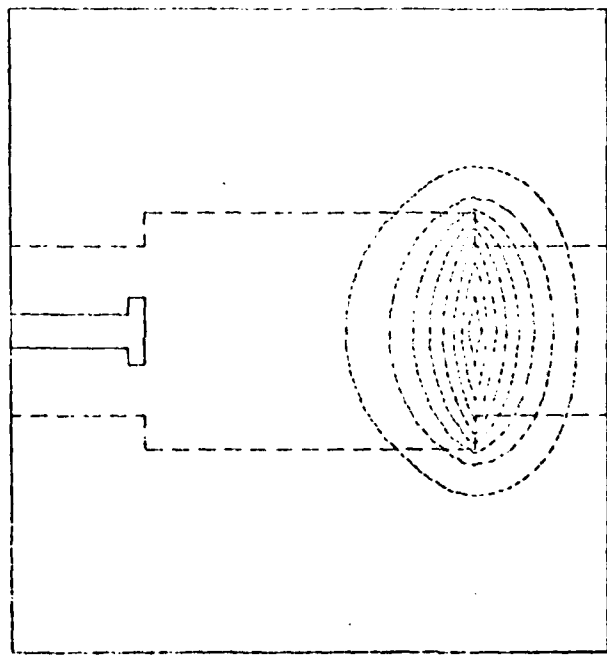
MINIMUM POTENTIAL
1KV2 , CHARGE 0
MAXIMUM POTENTIAL
1KV1 , CHARGE 6
CHARGE DENSITY IN FUEL
CHARGE DISTRIBUTION ON FORM
FILLING LEVEL
CONTUR SPACING



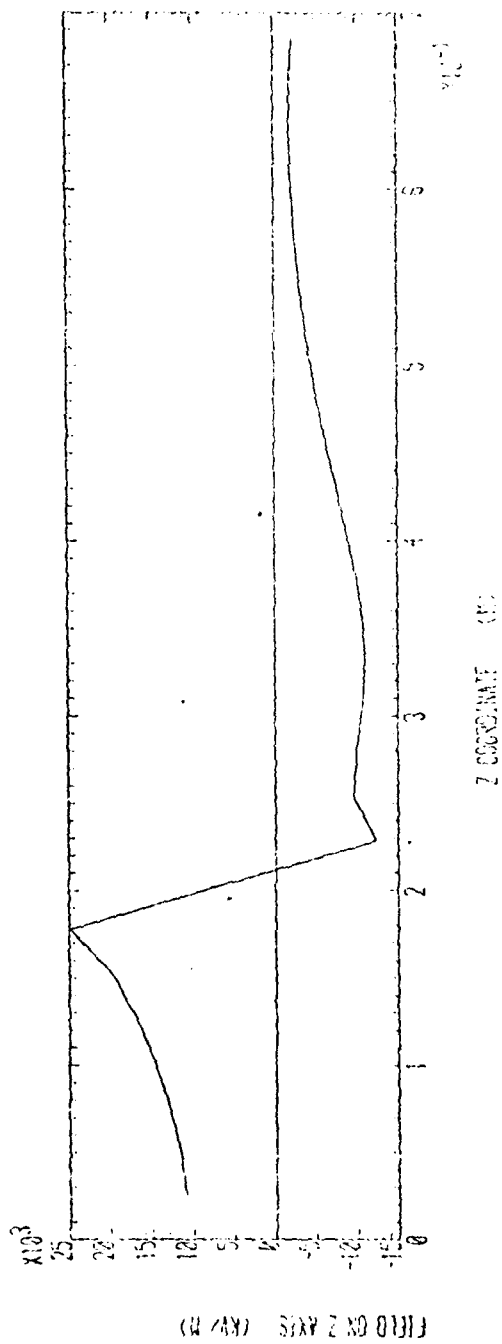
PLOT 5

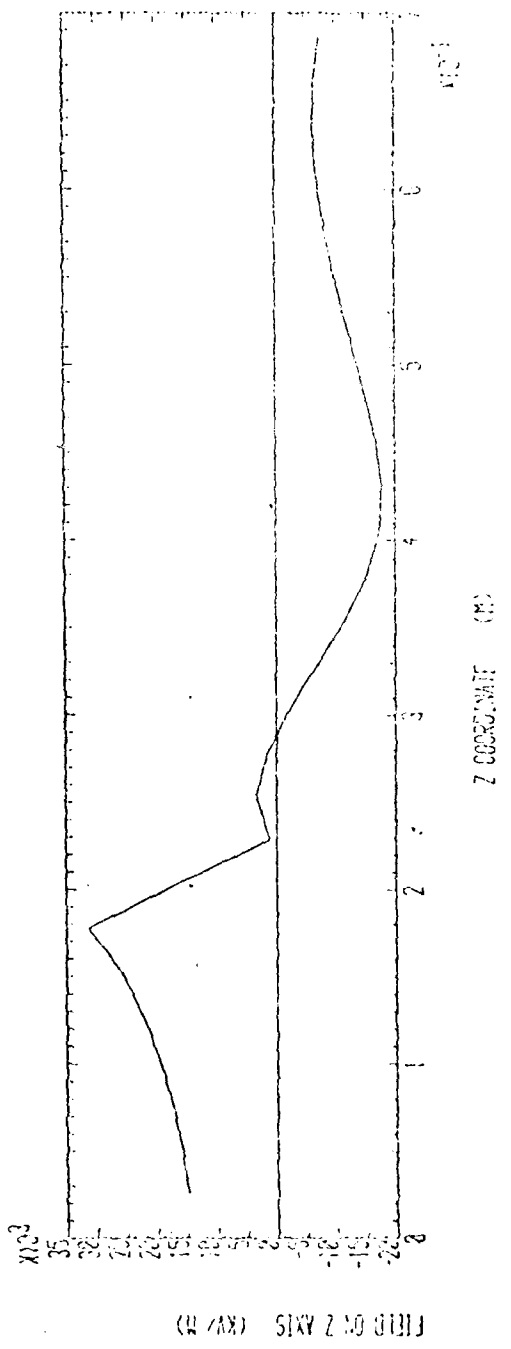


MINIMUM POTENTIAL 0KV
MAXIMUM POTENTIAL 1KV
CHARGE DENSITY IN FUEL 1C/m³.2003E-4
CHARGE DISTRIBUTION ON FOAM 1C/m³.1233E-2
FILLING LEVEL .010 .2003E-2
CONDUCTIVE SPACING 0KV 1.258E-6



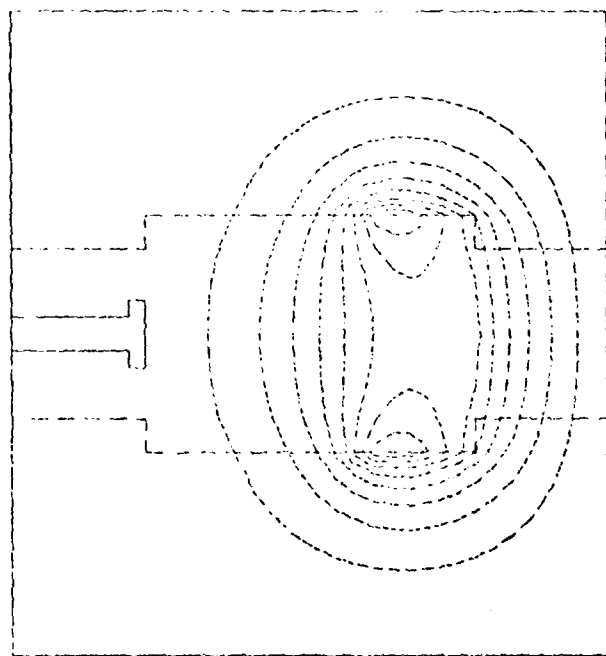
PLOT 6

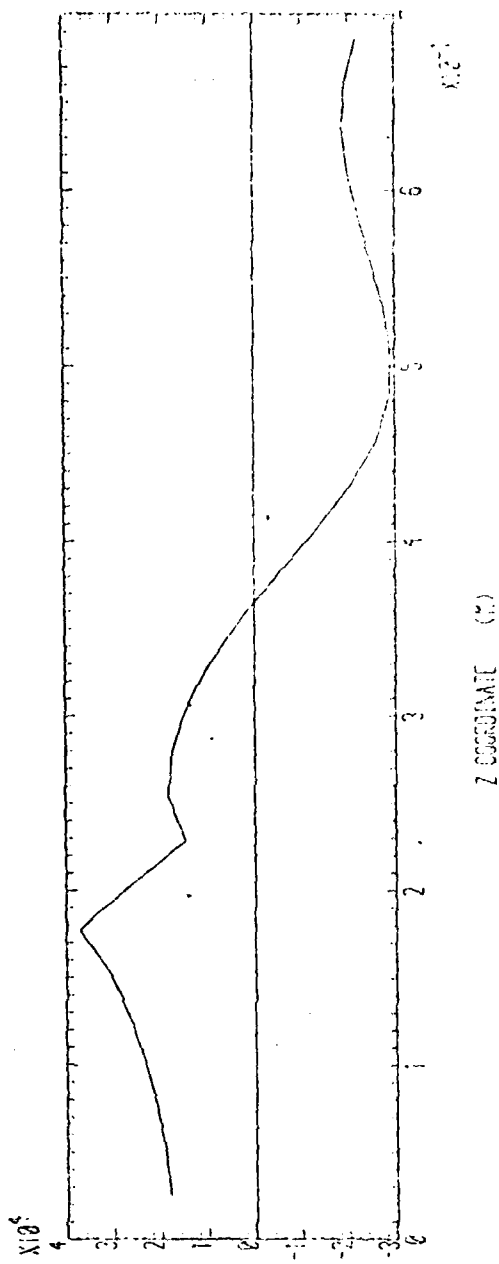




(U//MX) SIXY 2 NO 00111

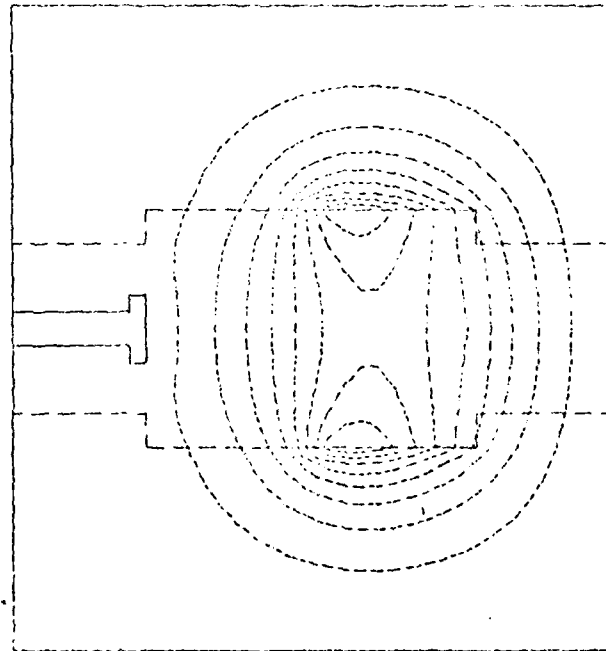
MATERIAL PROPERTIES
MAXIMUM STRESS, MPa
GRANULAR DENSITY IN TONS
GRAIN DISTRIBUTION ON PEGAP
FLUID LEVEL
CONTOUR SPACING



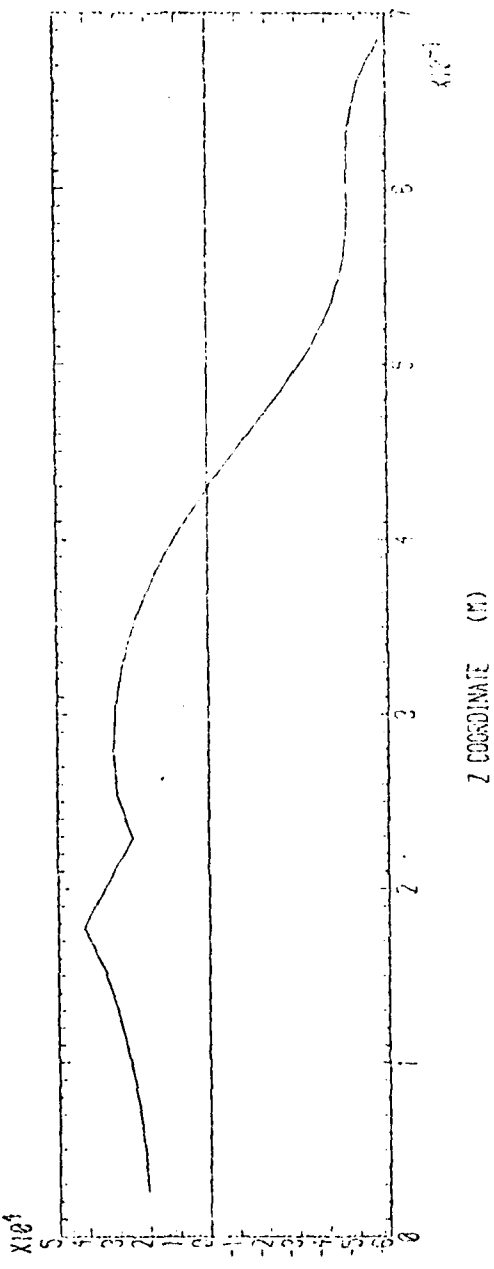


(W/AB) SIN X NO OTHER

MINIMUM POTENTIAL 0.0000
 MAXIMUM POTENTIAL 0.0000
 CHARGE DENSITY IN FOC 0.0000
 CHARGE DISTRIBUTION ON FOC 0.0000
 FILLING LEVEL 0.0000
 CONTROL OF BEAMS 0.0000

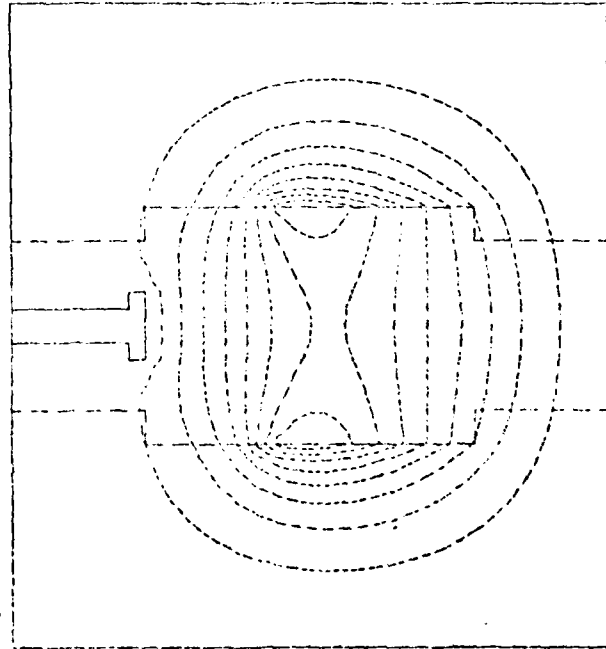


PLOT 9

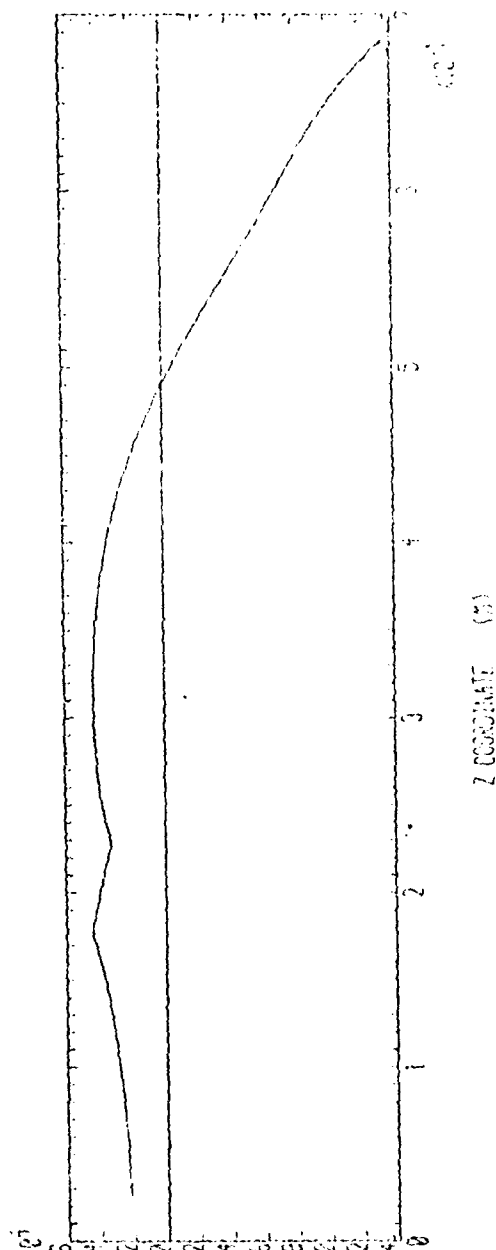


(W/AN) SIXY Z NO 0711

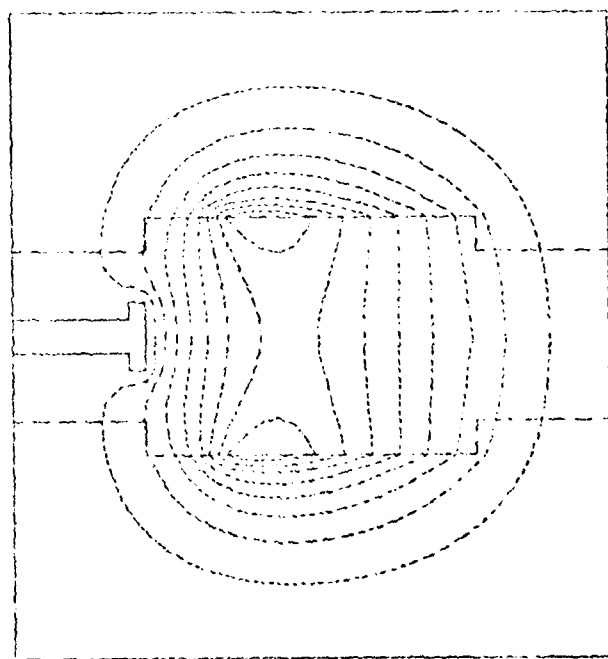
MINIMUM POTENTIAL. 1895.0000E-0
 MAXIMUM POTENTIAL. 1895.1142E-0
 CHARGE DENSITY IN FILE. 10000.0000E-0
 CHARGE DISTRIBUTION ON FDAT. 10000.0000E-0
 FILLING LEVEL. 100.0000E-0
 CONTOUR SPAC, NC. 1895.0000E-0



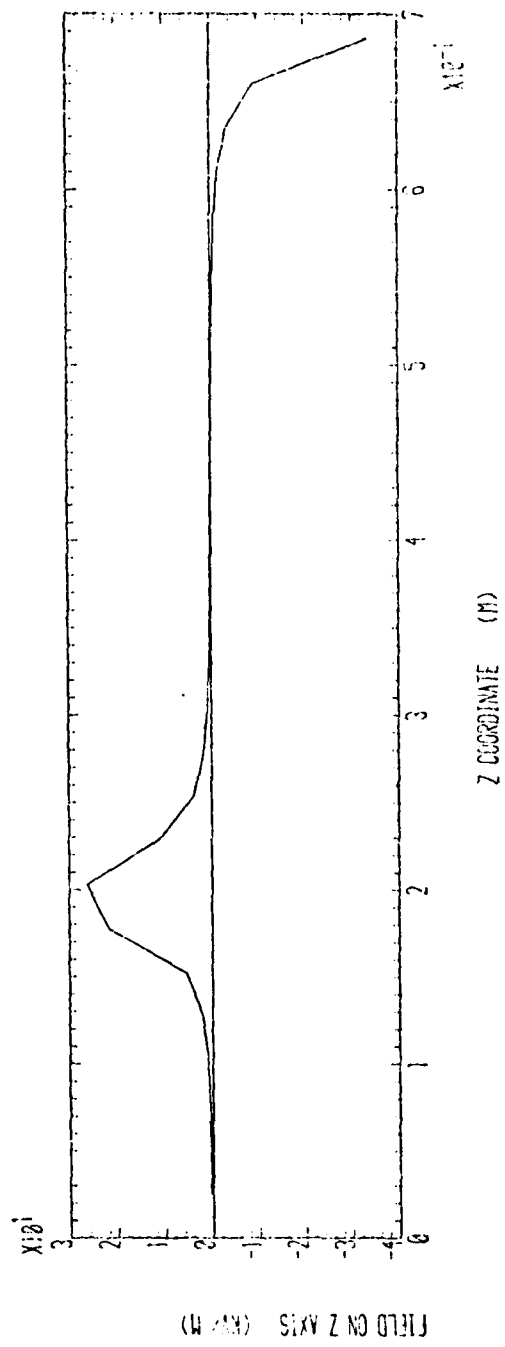
PLOT 10



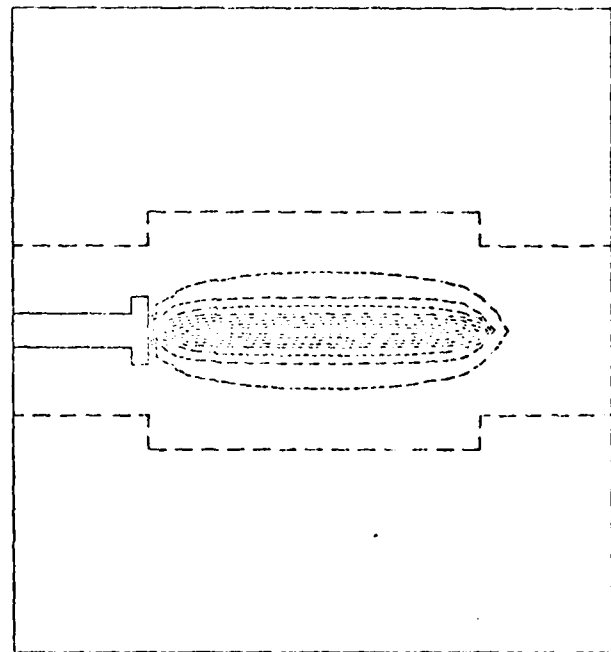
(U//AX) SIXX Z NO 07313



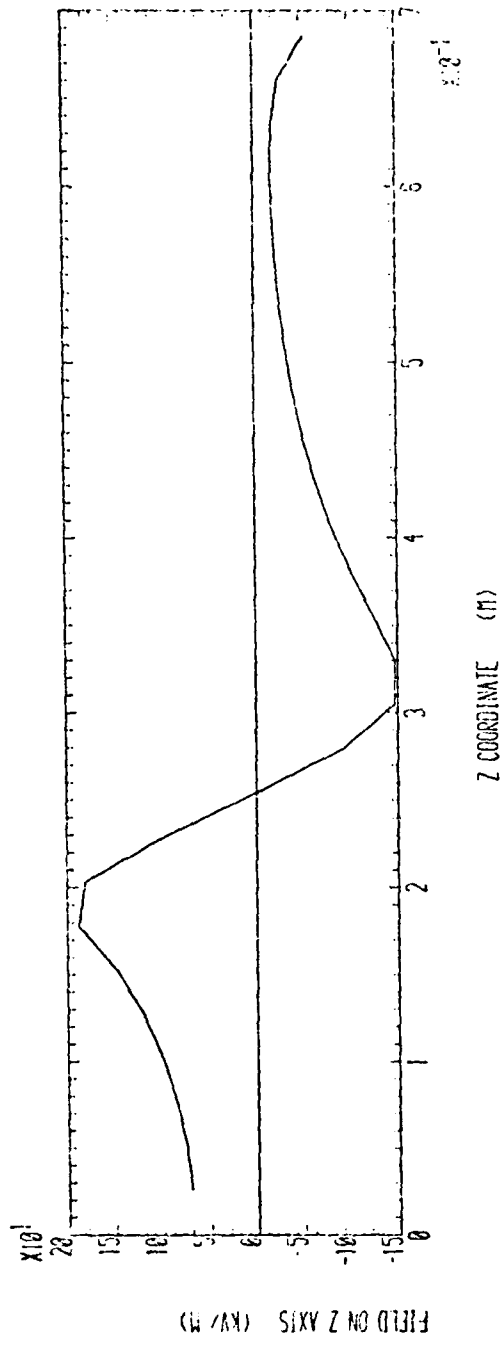
PLOT 11



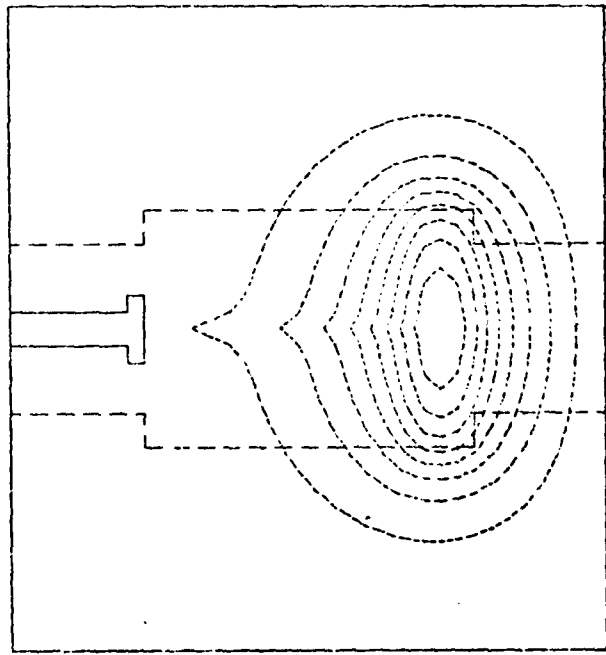
MINIMUM POTENTIAL	1KV .000E 0
MAXIMUM POTENTIAL	1KV .188E 4
CHARGE DENSITY IN FUEL	CHARGE .1232E -3
CHARGE DISTRIBUTION ON FOAM	CHARGE .3333E 3
FILLING LEVEL	FILL .000E 0
CONTOUR SPACING	CKV .2165E 3



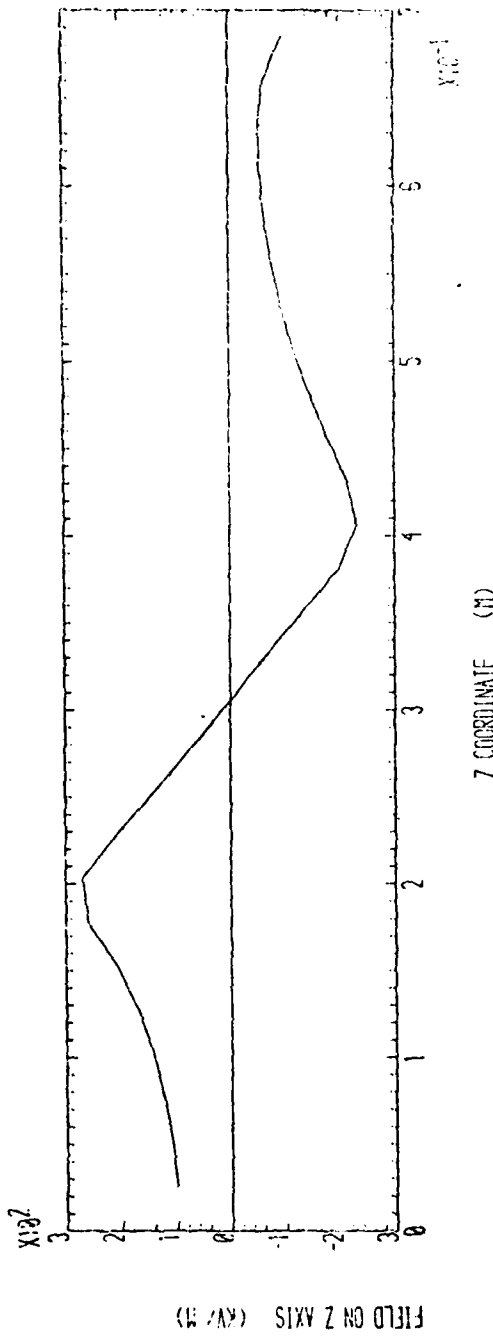
PLOT 12



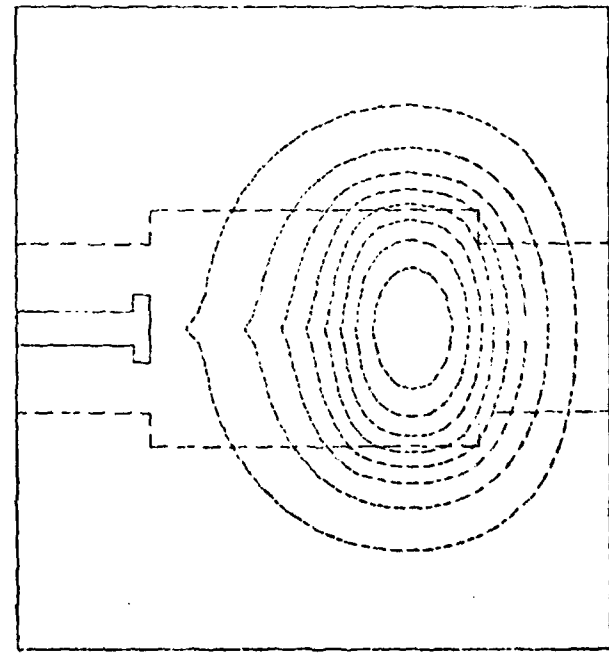
MINIMUM POTENTIAL	1.0000	0
MAXIMUM POTENTIAL	1.0000	0
CHARGE DENSITY IN FUEL	1.0000	-3
CHARGE DISTRIBUTION ON FCAM	1.0000	0
FILLING LEVEL	0.0000	0
CONTOUR SPACING	0.0000	+



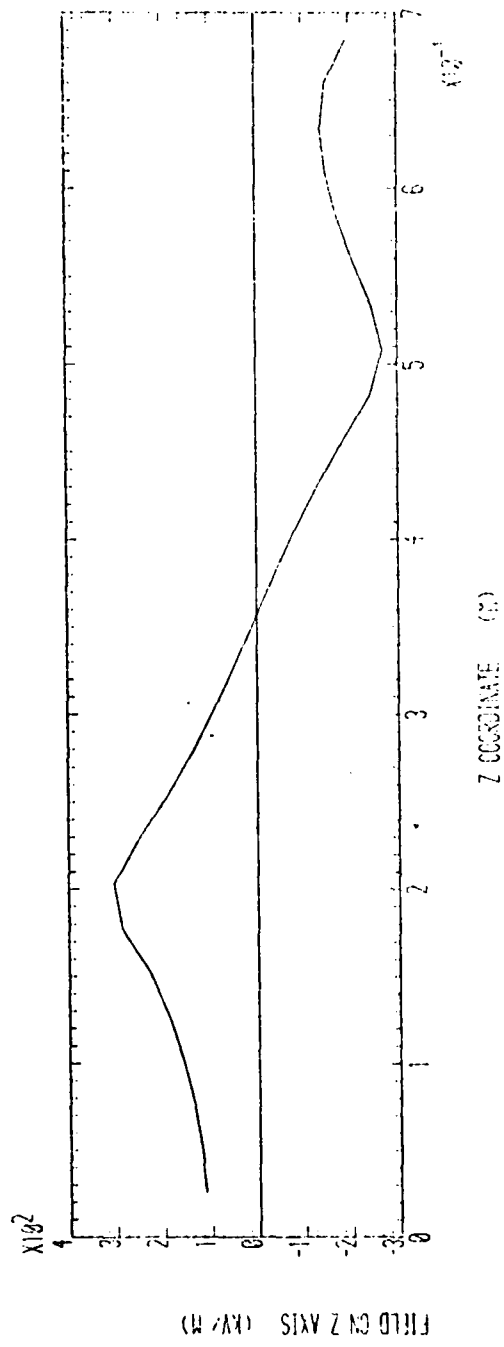
PLOT 13



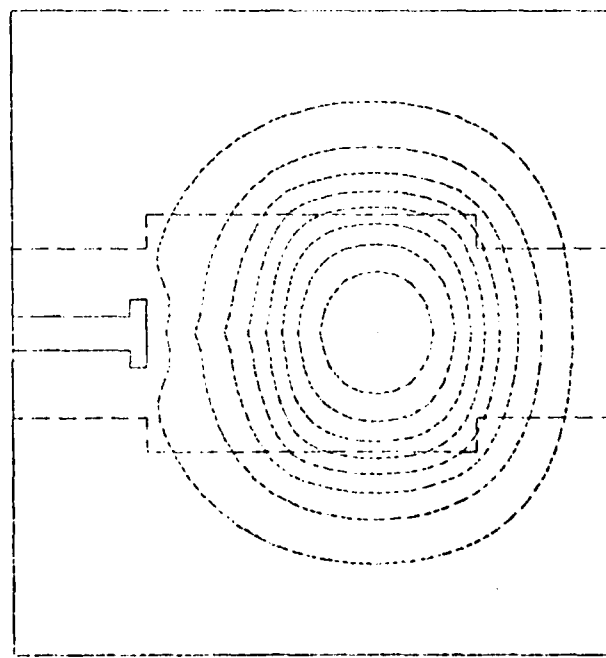
MINIMUM POTENTIAL	[KVJ .0333E -2
MAXIMUM POTENTIAL	[KVJ .4722E -3
CHARGE DENSITY IN FUEL	[C/MM3] .1333E -3
CHARGE DISTRIBUTION ON FOAM	[C/MM3] .0222E -2
FILLING LEVEL	(M) .00033
CONTOUR SPACING	[KVJ .5246E -4



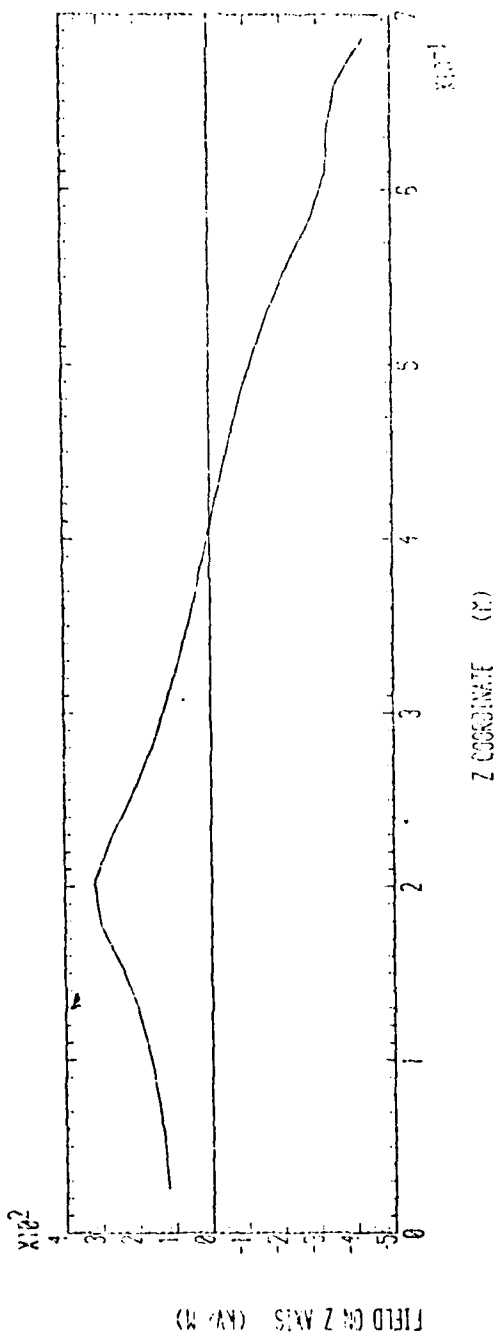
PLOT 14



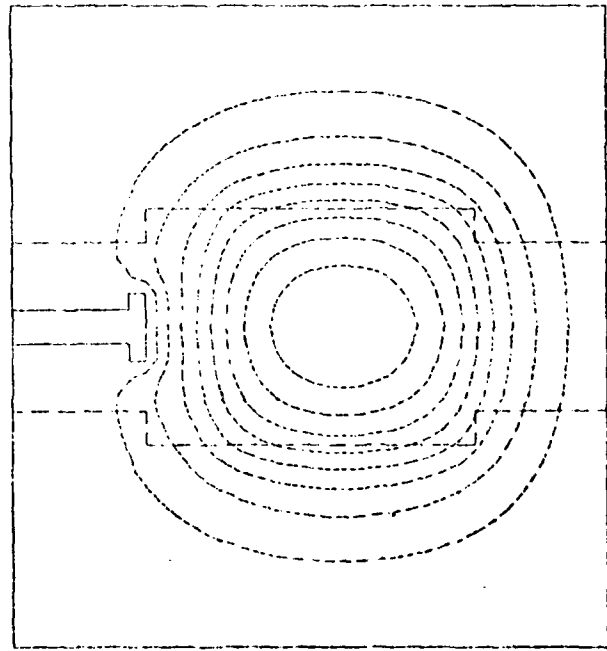
MINIMUM POTENTIAL	0.8MV
MAXIMUM POTENTIAL	1.8MV
CHARGE DENSITY IN FUEL	0.013C/cm ³
CHARGE DISTRIBUTION ON FOAM	0.002C/cm ³
FILLING LEVEL	0.85M
CONTOUR SPACING	0.05M



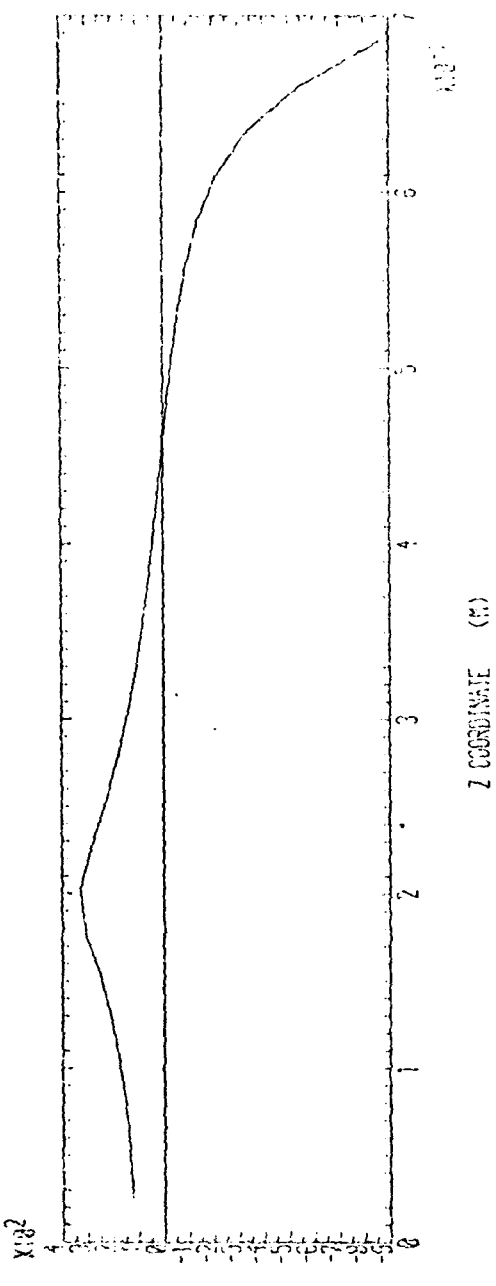
PLOT 15



MINIMUM POTENTIAL	-5.00	MAXIMUM	5.00
MAXIMUM POTENTIAL	6.775E-05	CHARGE DENSITY	0.000E+00
CHARGE DENSITY IN FUEL	0.000E+00	CHARGE DISTRIBUTION ON FOAM	0.000E+00
FILLING LEVEL	0.000E+00	CONCURRENCE	0.000E+00
CONCURRE SPACING	0.000E+00		

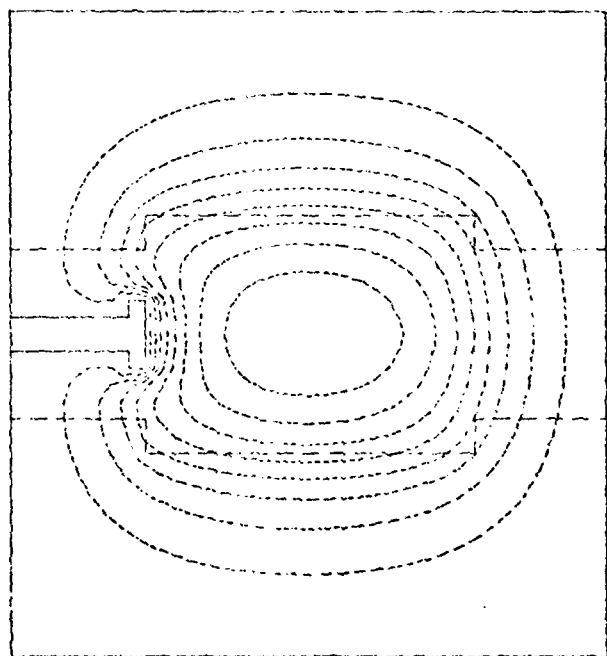


PLOT 16



(U) (R) SIX Z NO 01113

MINIMUM POTENTIAL 1KV
 MAXIMUM POTENTIAL 3KV
 CHARGE DENSITY IN FUEL 1000
 CHARGE DISTRIBUTION ON FUEL 1000
 FILLING LEVEL 0.25
 CONTOUR SPACING 4



PLOT 17

PLOTS 18 - 30

The configuration for plots 18 - 30 consists of foam Section 4 together with foam Sections 1 and 2 inserted. (See Figure 7).

Plots 18 - 22 Charge density in fuel = 10^{-4} C/m³

Charge density on foam surface = 0 C/m²

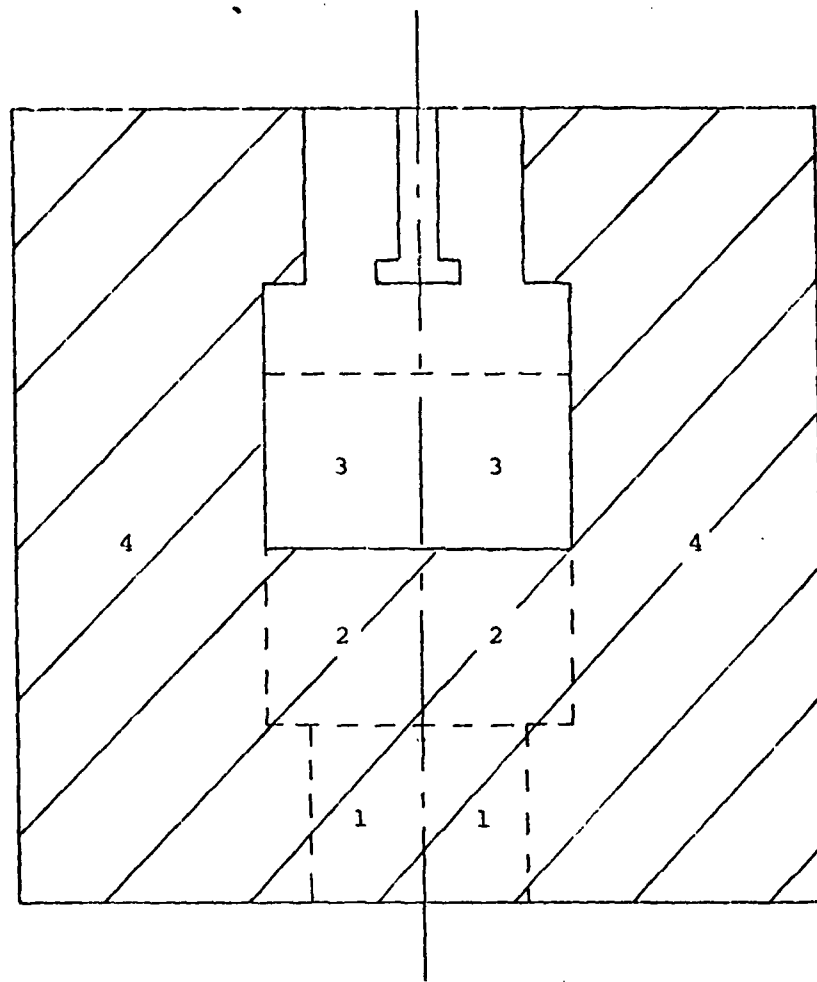
Filling levels at .1, .2, .3, .4, .5 metres
above base.

Plot 23 Surface charge density of 10^{-3} C/m² on Section 2
upper surface only.

Plots 24 - 26 Surface charge on Section 2 upper surface and at
heights .1, .2, .3 metres above this surface.

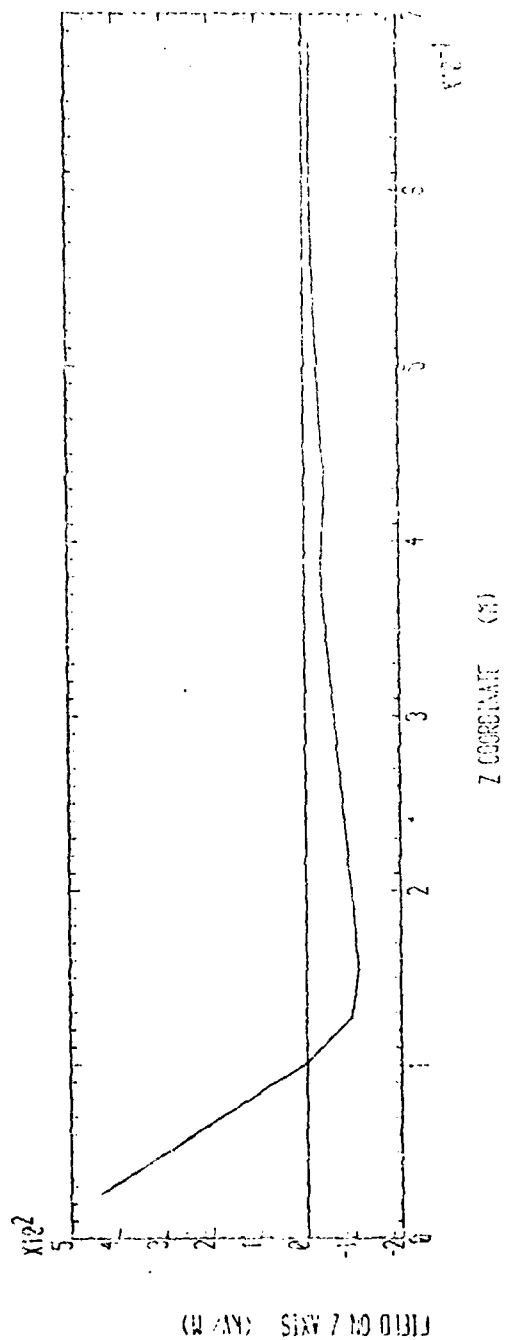
Plot 27 Vertical stream of fuel with charge density
 10^{-4} C/m³ impinging on the target area.

Plots 28 - 30 Vertical stream of fuel + voiding region filled
to heights .1, .2, .3 metres.

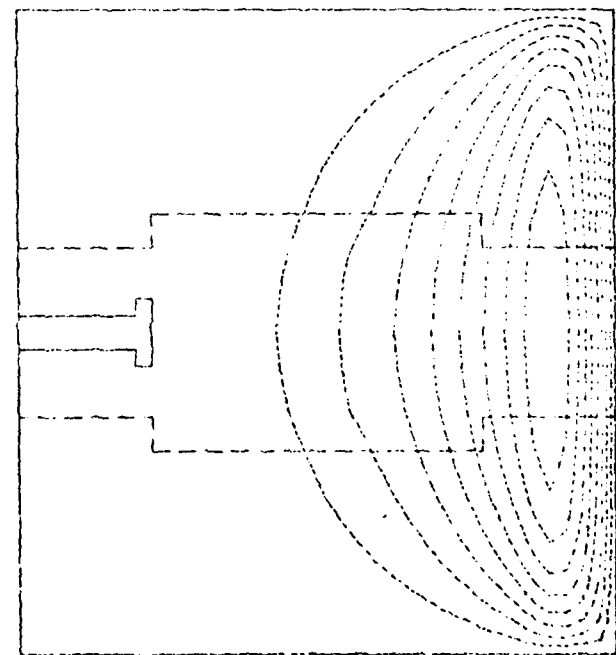


Foam sections 1 , 2 , and 4 in place

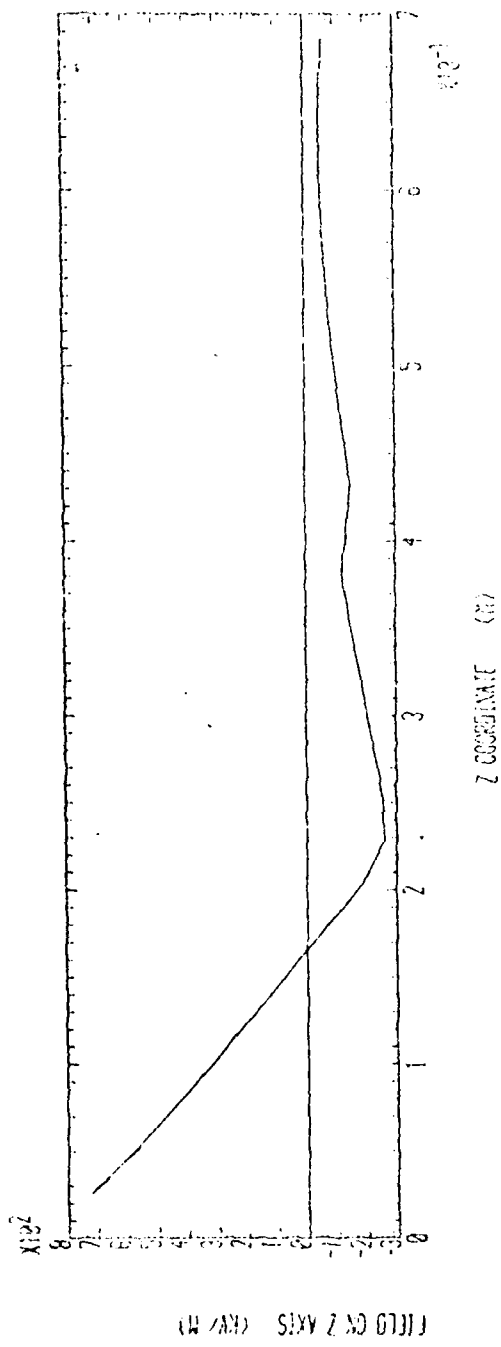
fig. 7.



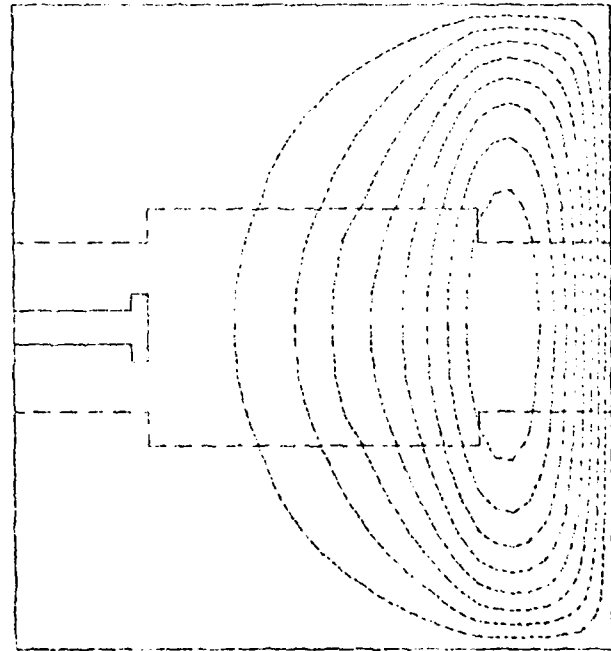
MINIMUM POTENTIAL : 0KV
 MAXIMUM POTENTIAL : 6KV
 CHARGE DENSITY IN FUEL : 100000 C/CM³
 CHARGE DENSITY ON FUEL : 100000 C/CM³
 FILLING LEVEL : 100%
 CONTOUR SPACING : 0.0005M



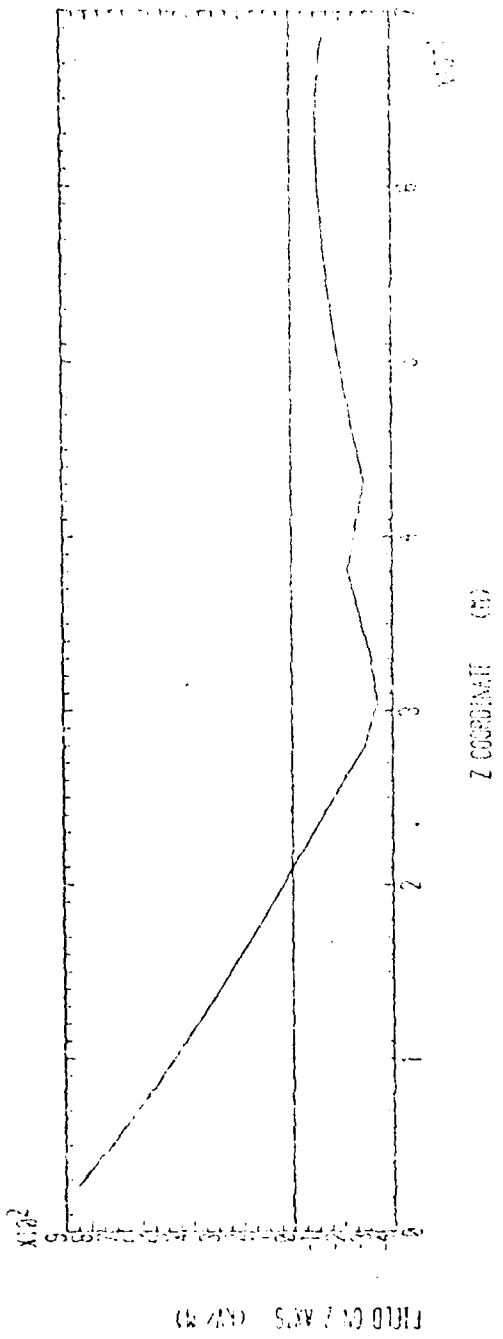
PLOT 18



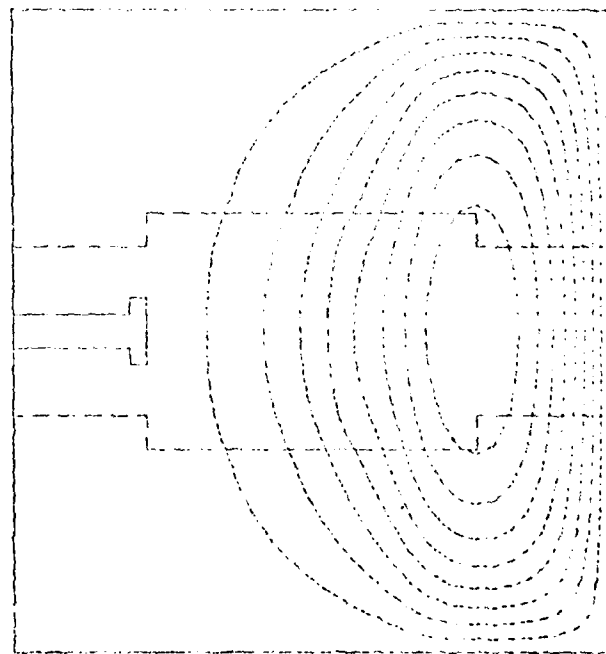
MINIMUM POTENTIAL 0.95
 MAXIMUM POTENTIAL 0.95
 CHARGE DENSITY IN TUBE 0.95
 CHARGE DENSITY ON PLATE 0.95
 FILMING LEVEL 0.95
 CONTOUR SPACING 0.95



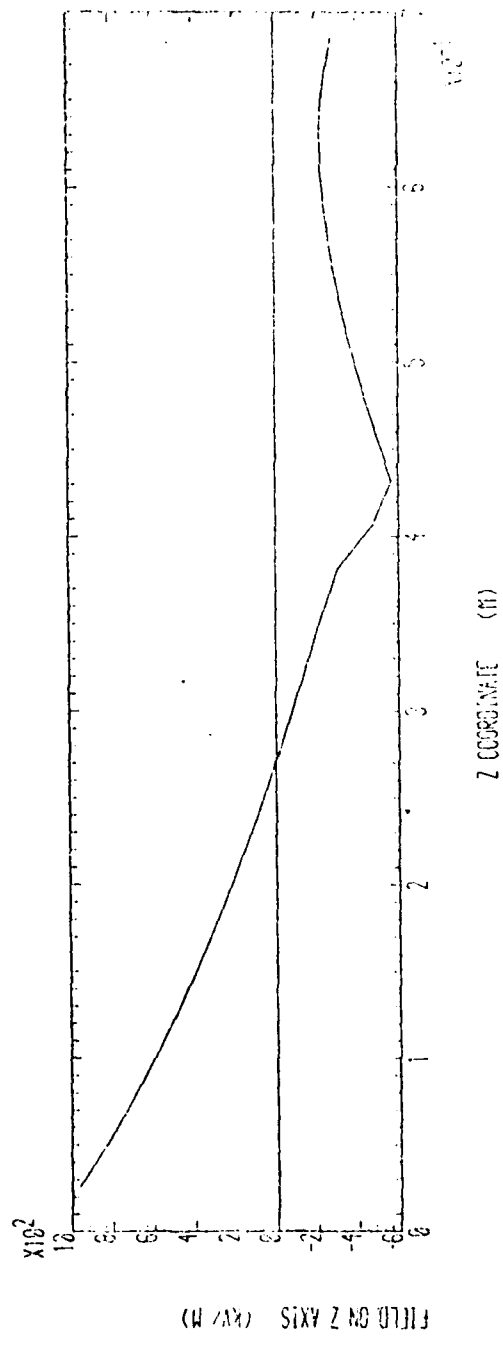
PLOT 19



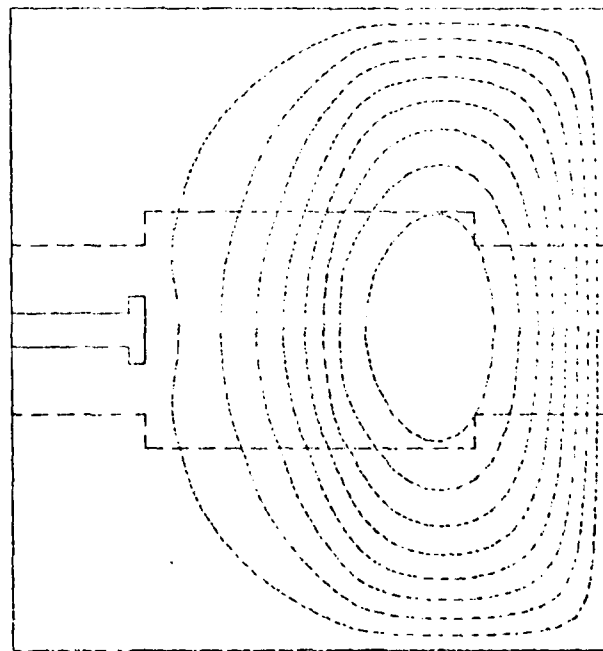
MAXIMUM POTENTIAL: 1600 VOLTS
 MAXIMUM FIELD: 1000 VOLTS/CM.
 CHARGE DENSITY IN FIELD: 1000 C/M³
 CHARGE DISTRIBUTION ON PLATE: 1000 C/M²
 FIELDING LEVEL: 1000 VOLTS
 SURFACE GRADIENTS: 1000 VOLTS/CM.



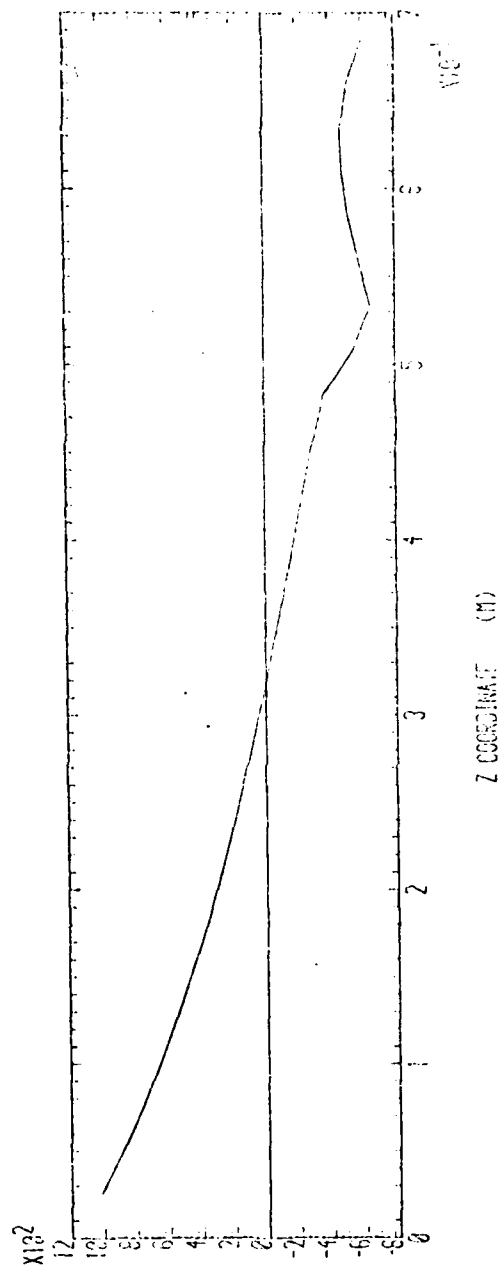
PLOT 20



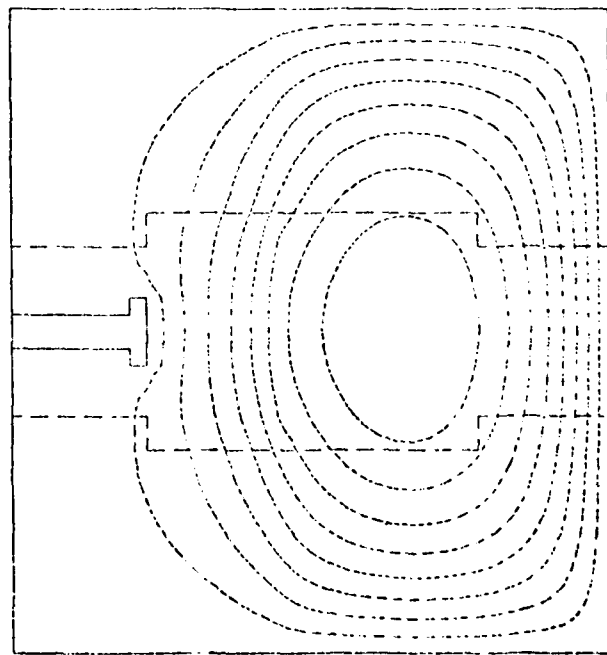
MINIMUM POTENTIAL 1.00
MAXIMUM POTENTIAL 0.00
CHARGE DENSITY IN FUEL 1.00E-03
CHARGE DISTRIBUTION ON FOAM 1.00E-03
FILLING LEVEL 1.00E-03
CONTOUR SPACING 0.00



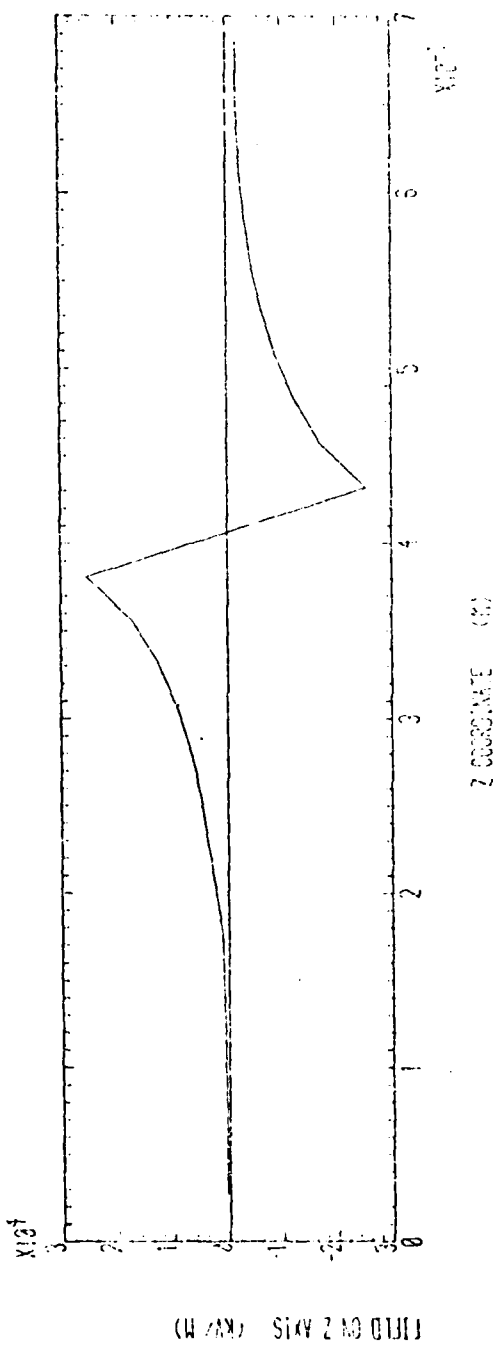
PLOT 21



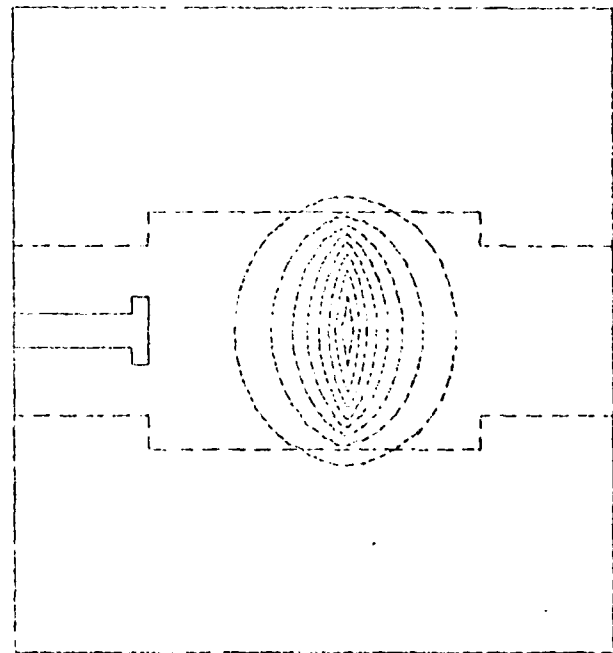
(W/M) SIXTY TWO



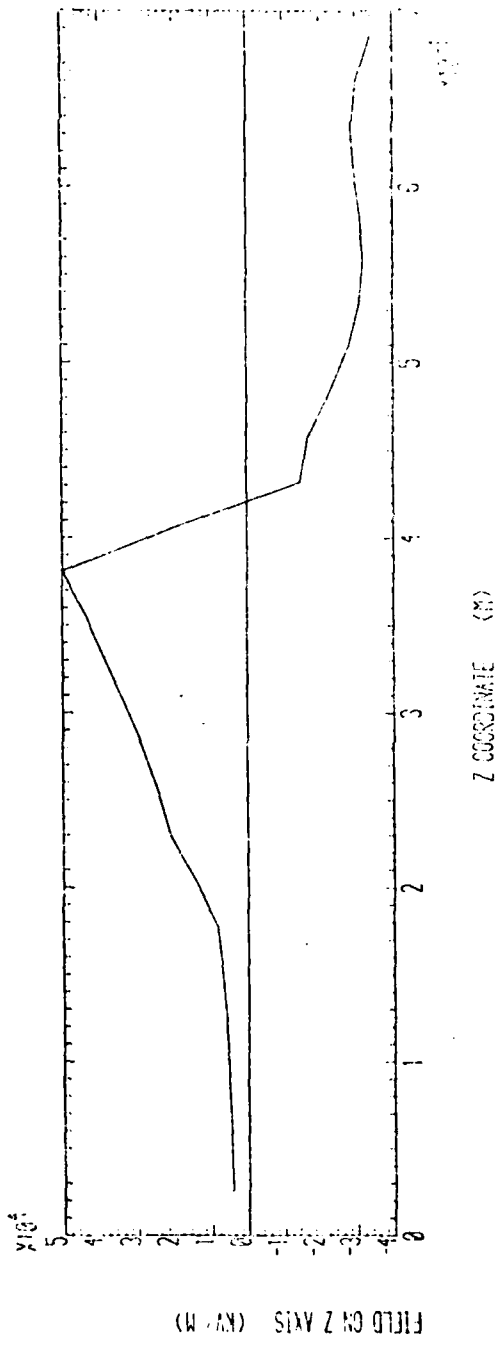
PLOT 22



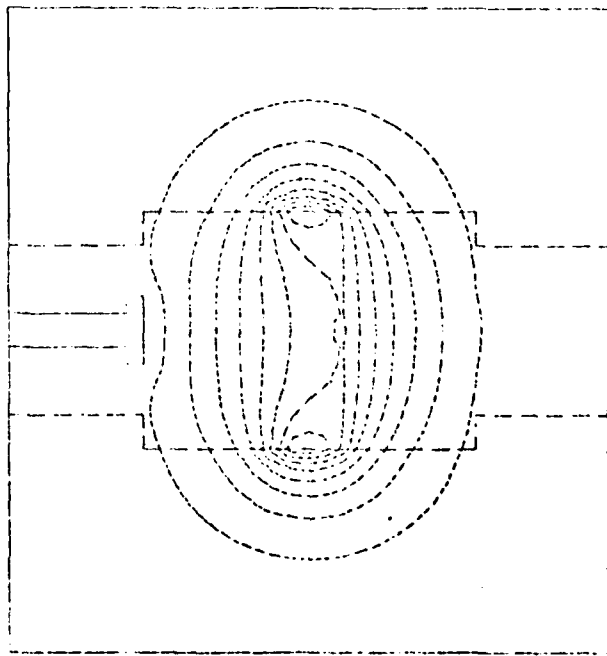
MINIMUM POTENTIAL (KV) 2000
 MAXIMUM POTENTIAL 2000
 CHARGE DENSITY IN FIELD 10000 ELECTRON
 CHARGE DISTRIBUTION FROM FINITE DIFFERENCE
 FILMING LEVEL 10000 ELECTRON
 CONTOUR SPACING 2000 ELECTRON



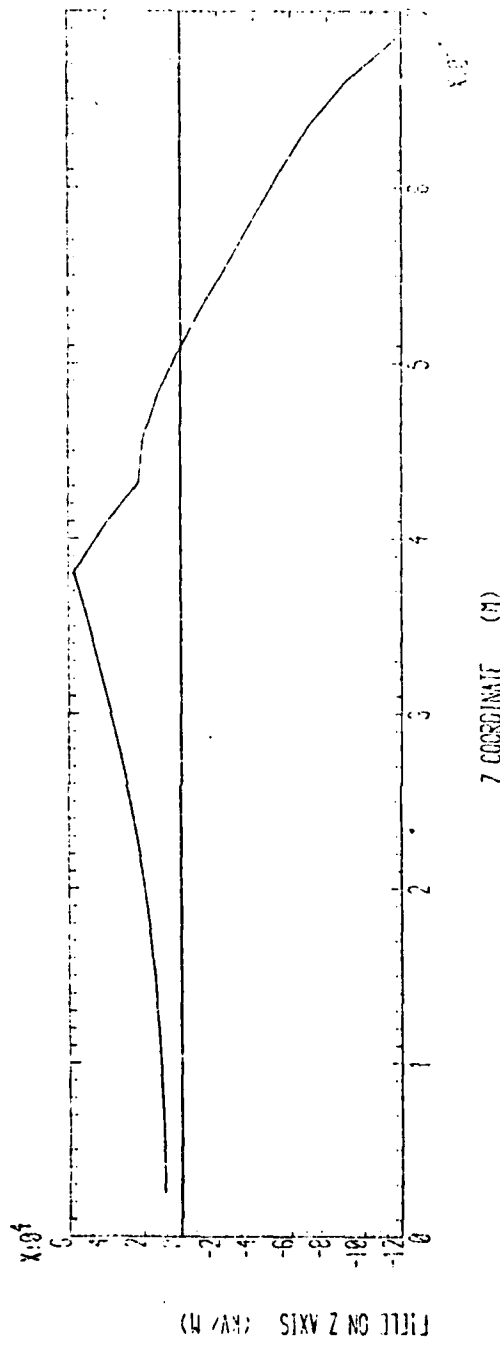
PLOT 23



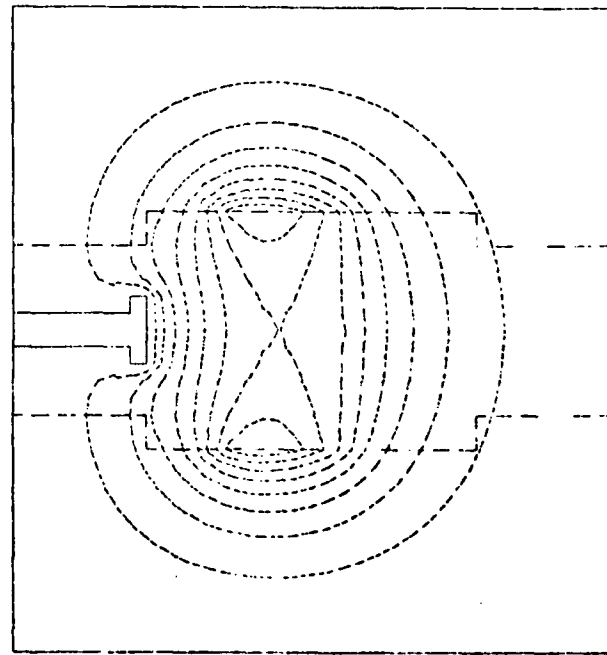
MINIMUM POTENTIAL	0.02 . 500KV
MAXIMUM POTENTIAL	.0.02 . 500KV
CHARGE DENSITY IN FUEL	10.433 . 200KV
CHARGE DISTRIBUTION ON FOAM	10.432 . 200KV
FILLING LEVEL	0.02 . 200KV
CORR. R. SPACING	0KV . 1147E



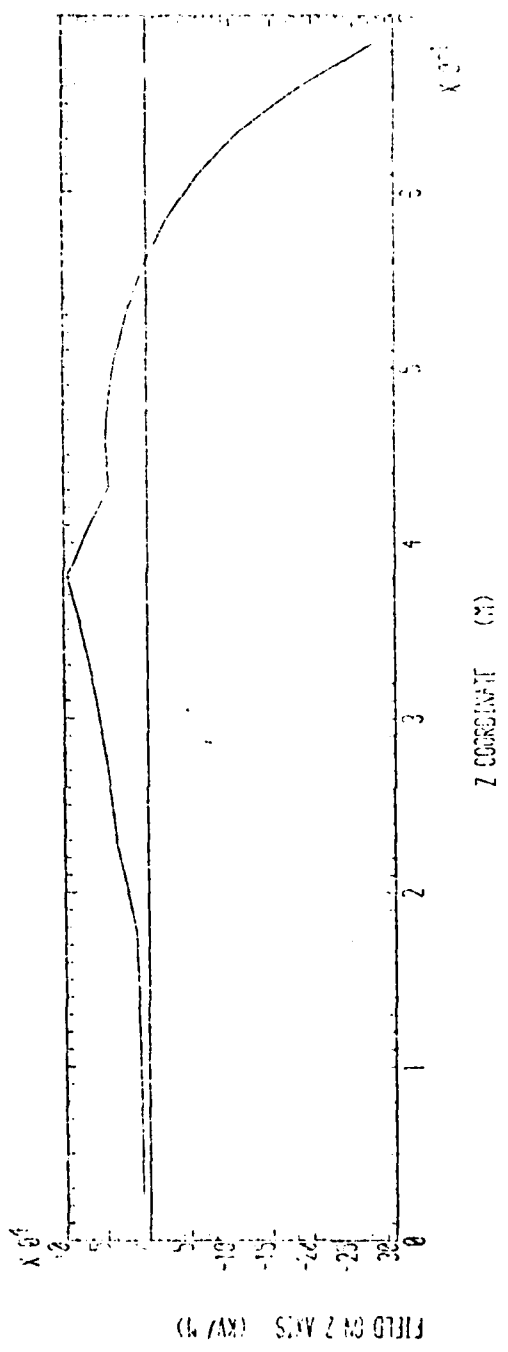
PLOT 24



MINIMUM POTENTIAL
MAX. DENSITY 0
MAX. POTENTIAL 6
CHARGE DENSITY IN FL 16.00000E-02
CHARGE DISTRIBUTION ON FOAM 1.00000E-02
FILLING LEVEL 0.00000E+00
CONTOUR SPACING 1.00000E-02

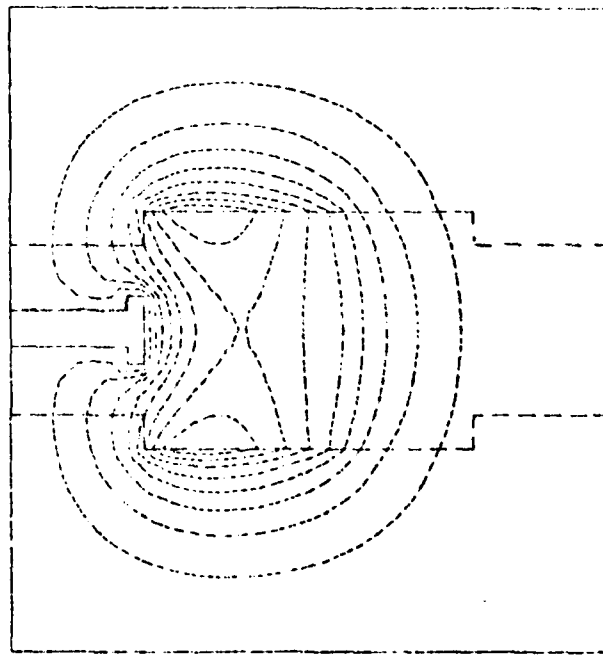


PLOT 25

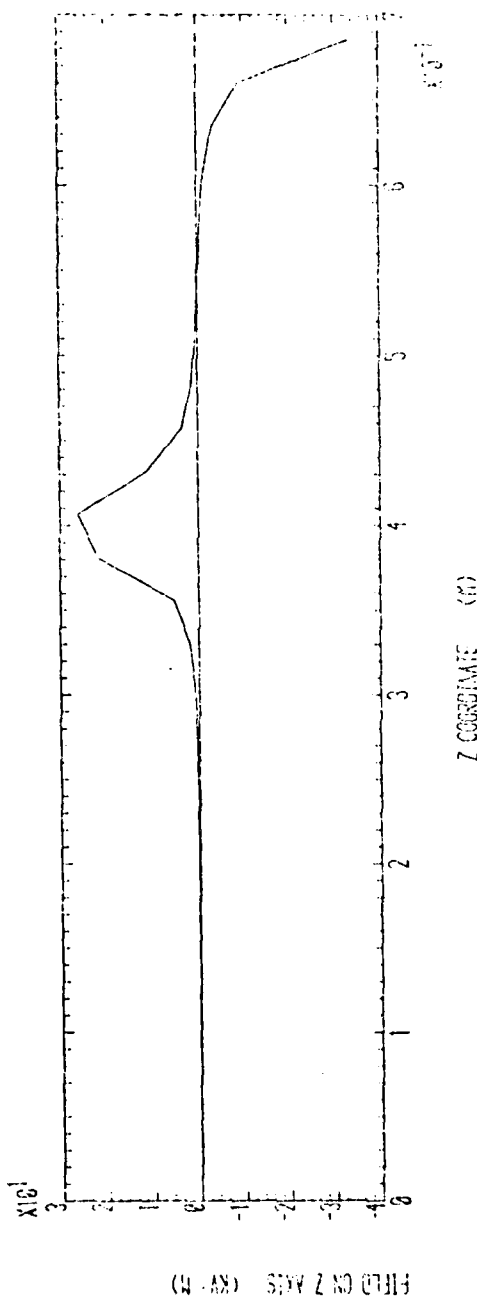


MINIMUM POTENTIAL
MAXIMUM POTENTIAL
CHARGE SENSITIVITY IN FUEL
CHARGE DISTRIBUTION ON FOAM
FILLING LEVEL
CONTIC IR SPACING

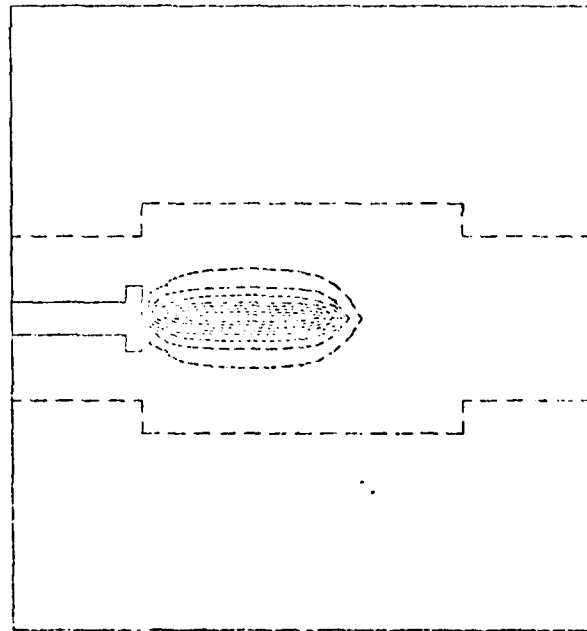
(KV) - SPACING 0
10KV - SPACING 0
10KV - SPACING 0
10KV - SPACING 0
10KV - SPACING 0
(KV) - SPACING 0



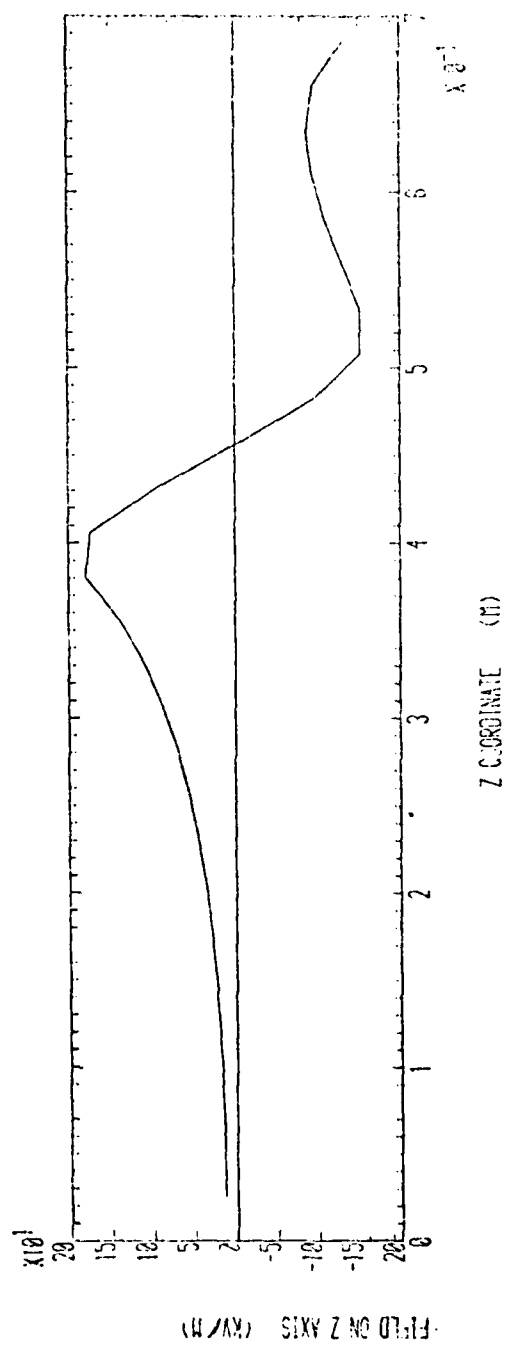
PLOT 26



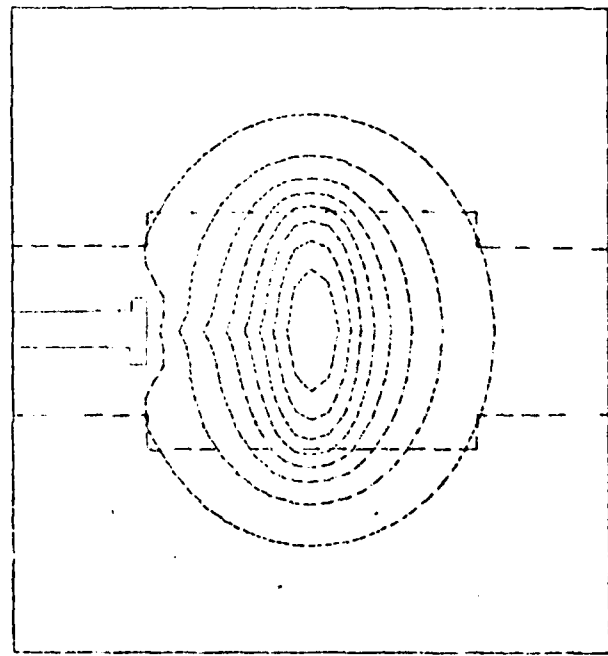
MINIMUM POTENTIAL	18.6	WEDGE	0
MAXIMUM POTENTIAL	18.6	WEDGE	4
CHARGE DENSITY IN FUEL	10.734	WEDGE	-3
CHARGE DISTRIBUTION ON FUEL	15.023	WEDGE	3
FILLING LEVEL	20.1	WEDGE	3
CONTOUR SPACING	18.6	WEDGE	3



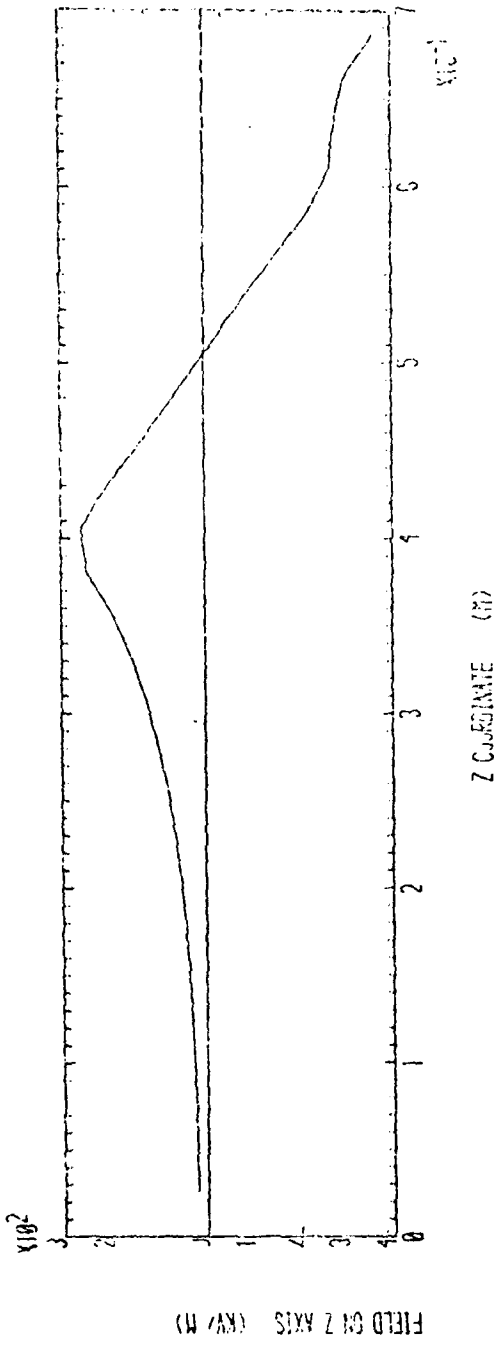
PLOT 27



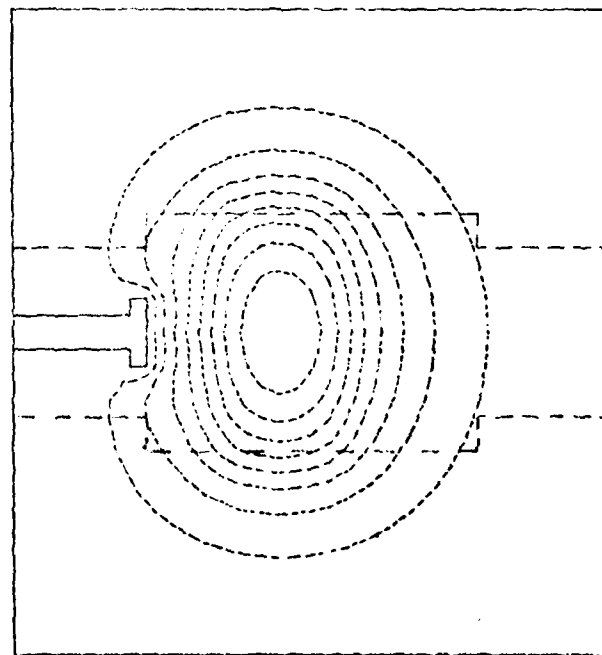
MINIMUM POTENTIAL	(KV) .0000 2
MAXIMUM POTENTIAL	(KV) .2335 5
CHARGE DENSITY IN FUEL	(C/M ³) 0.0E+0
CHARGE DISTRIBUTION ON FCAN	(C/M ³) 0.0E+0
FILLING LEVEL	.183 .000E 0
CONTOUR SPACING	(KV) .32556 4



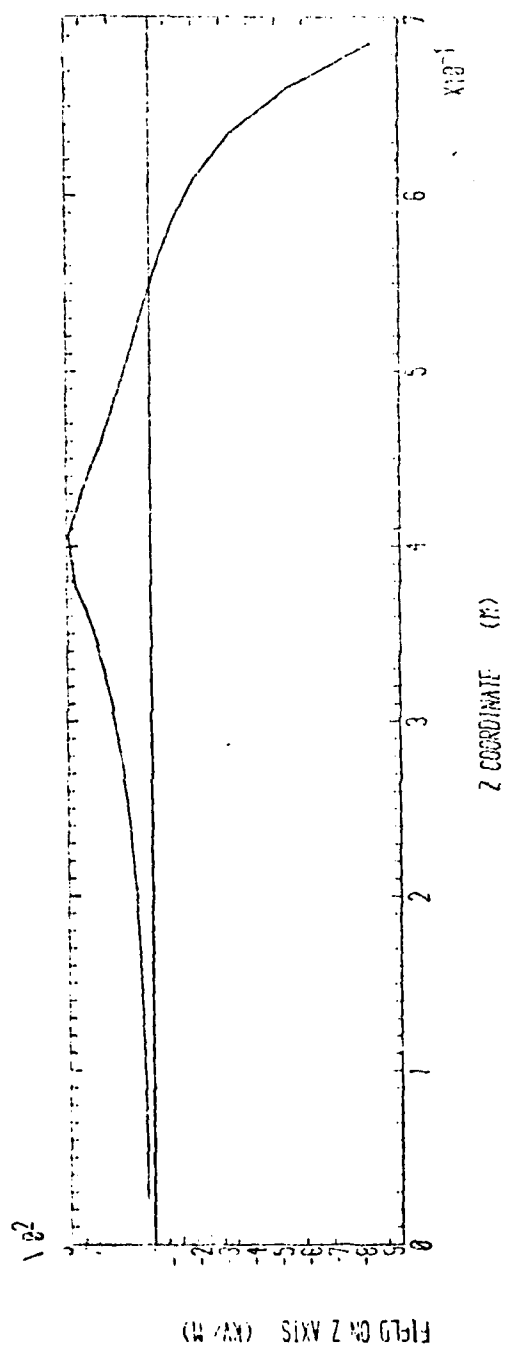
PLOT 28



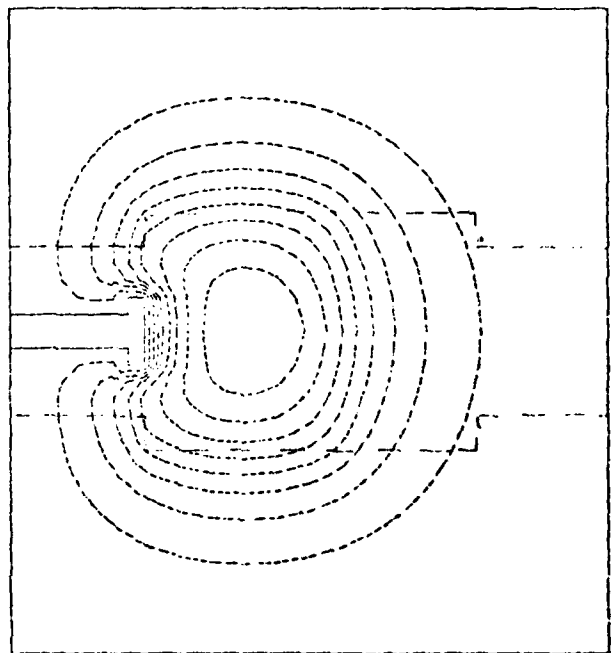
MINIMUM POTENTIAL 1KV .300E 0
 MAXIMUM POTENTIAL 1KV .4743E 0
 CHARGE DENSITY IN FUEL 0.0002 -3
 CHARGE DISTRIBUTION ON FUEL 0.0001 .000E 0
 FILLING LEVEL 1E .000E 0
 CONTOUR SPACING 1KV .5201E 0



PLOT 29



MINIMUM POTENTIAL	1.811 .0000E 0
MAXIMUM POTENTIAL	1.811 .5535E 5
CHARGE DENSITY IN E1	1.0 .1334E -2
CHARGE DISTRIBUTION ON FOAM	1.0 .20 00 E 0
FILLING LEVEL	1.0 .2033E 0
CONTROLLER SPACING	1.0 .6667E 4



PLOT 30

PLOTS 31 - 39

The configuration for plots 31-39 consists of foam Section 4 together with foam Sections 1, 2, and 3 inserted. (See Figure 8).

Plots 31 - 35

Charge density in fuel = 10^{-4} C/m³

Charge density on foam surface = 0 C/m²

Filling levels at .1, .2, .3, .4, .5 metres above base.

Plot 36

Surface charge density of 10^{-3} C/m² on Section 3

upper surface only.

Plot 37

Surface charge on Section 3 upper surface and at

height .1 metre above this surface.

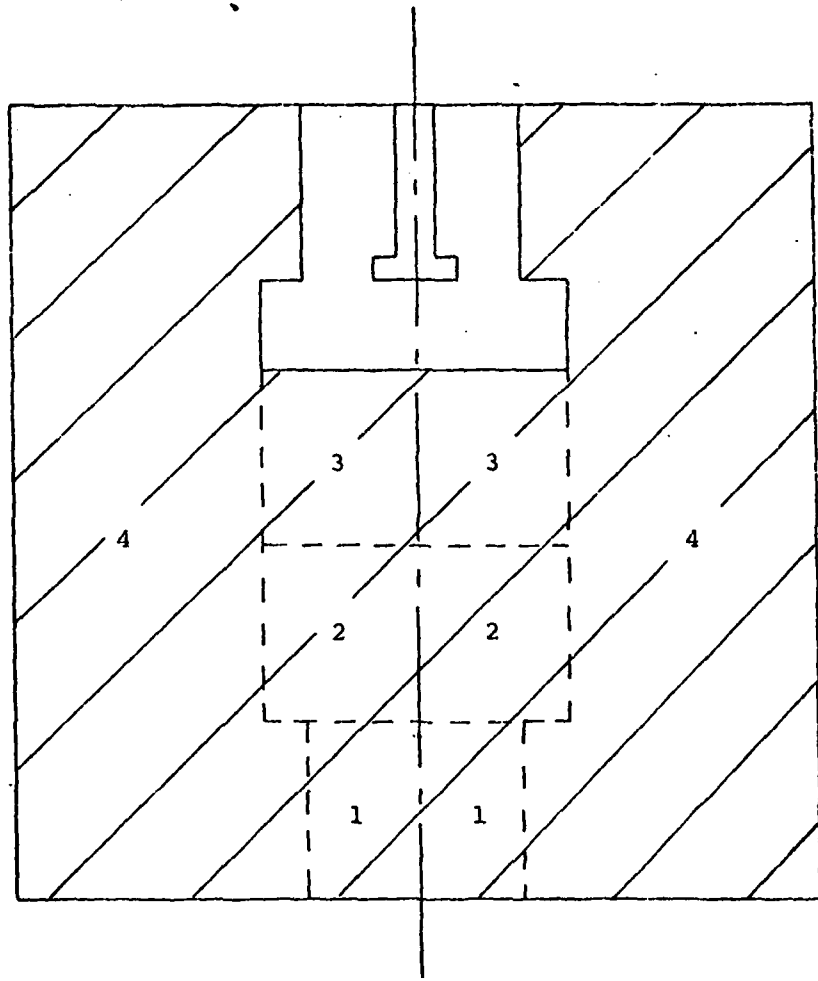
Plot 38

Vertical stream of fuel with charge density 10^{-4} C/m³

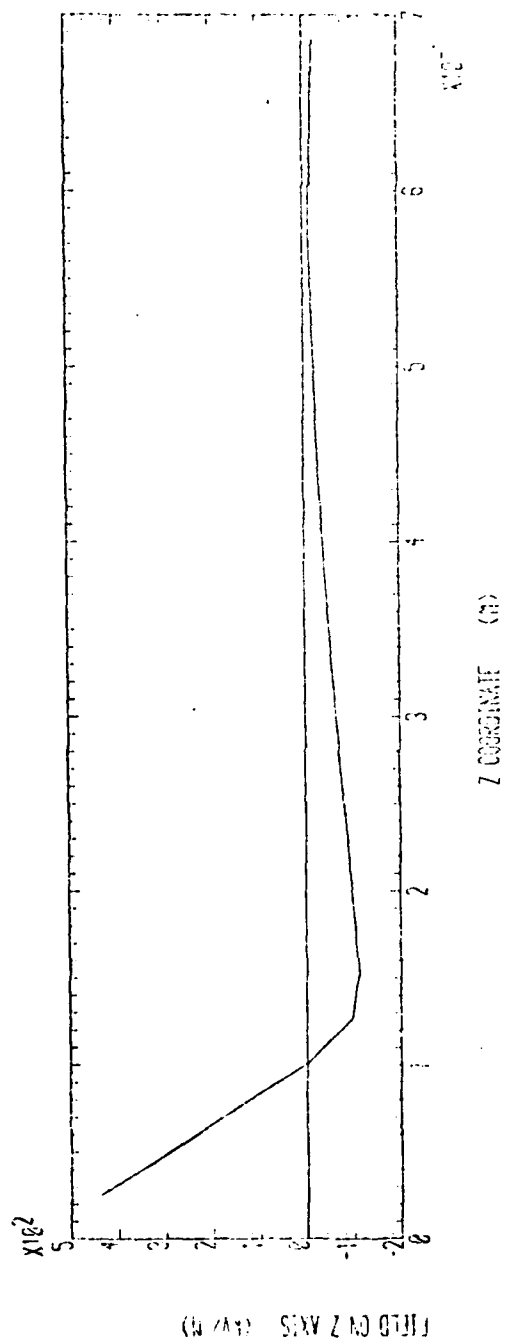
impinging on the target area.

Plot 39

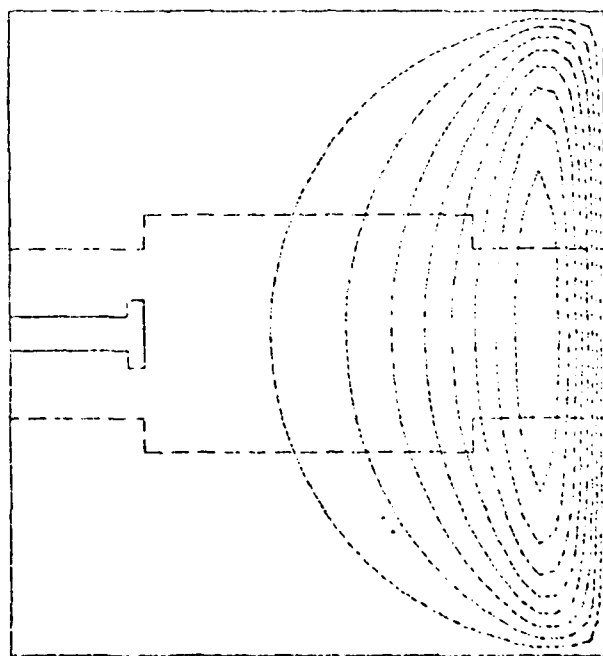
Voiding region filled with fuel.



Foam sections 1 , 2 , 3 , and 4 in place fig. 8.



MAXIMUM POTENTIAL	6KV ACROSS
MAXIMUM POTENTIAL	6KV ACROSS
CHARGE SENSITIVITY IN FIELD	1000, 10000
CHARGE DISTRIBUTION ON FOAM	1000, 10000
FILLING LEVEL	100, 1000
CONIGUR SPACING	1000, 10000



PLOT 31

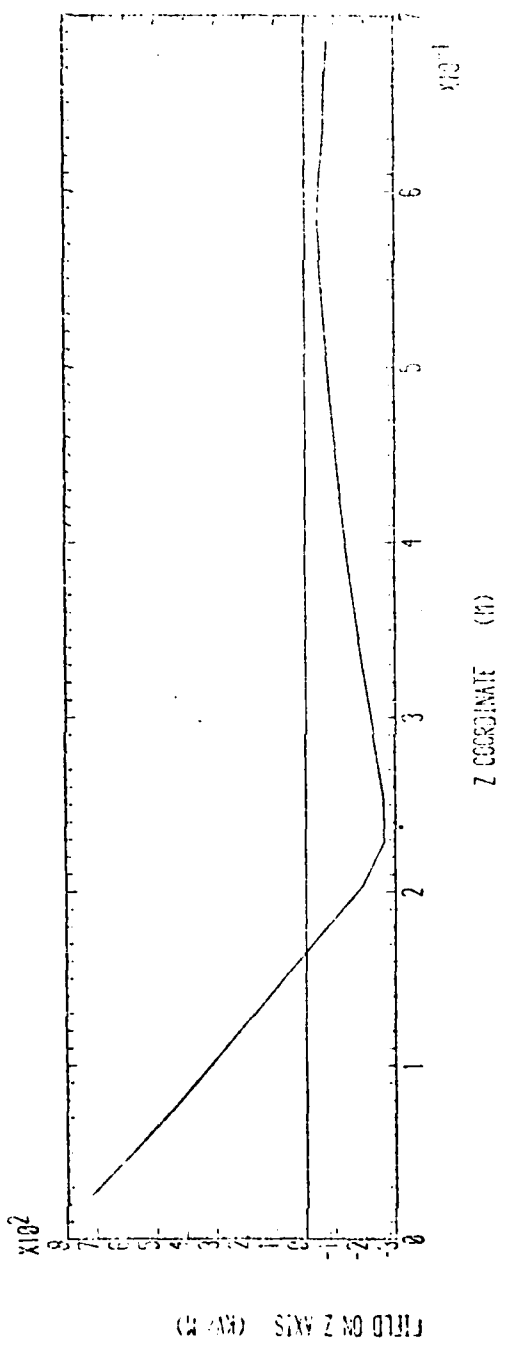
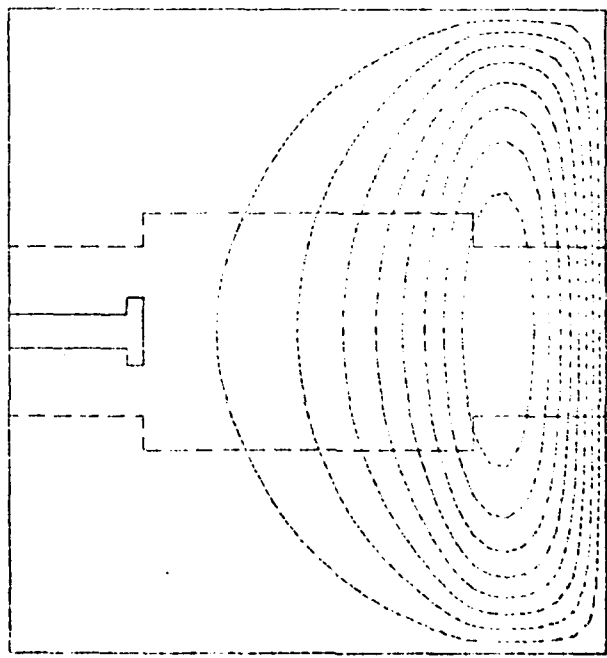
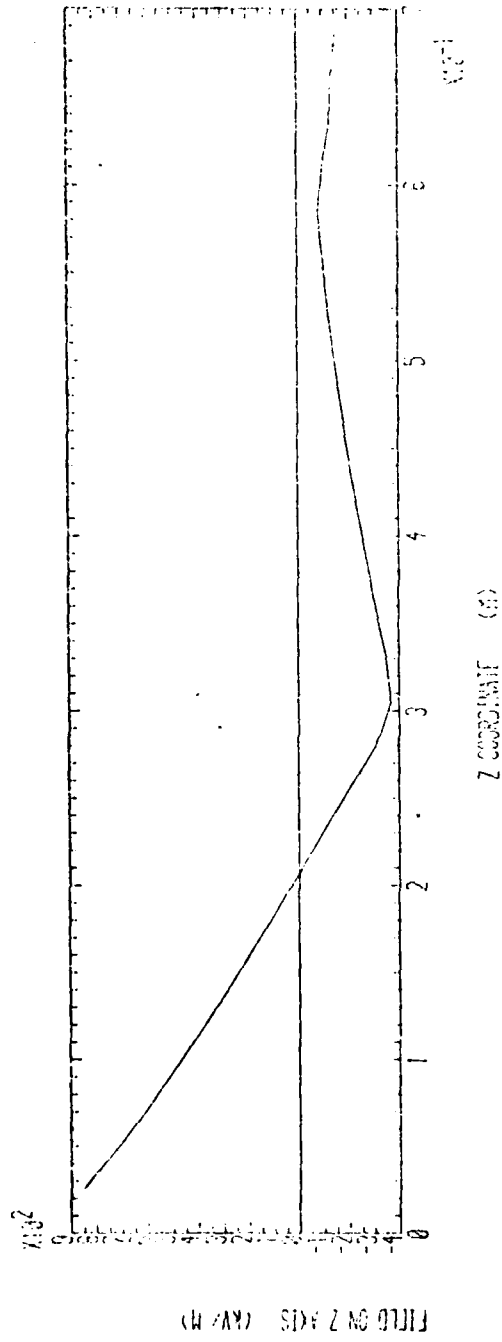


FIGURE SIX Z NO 0101

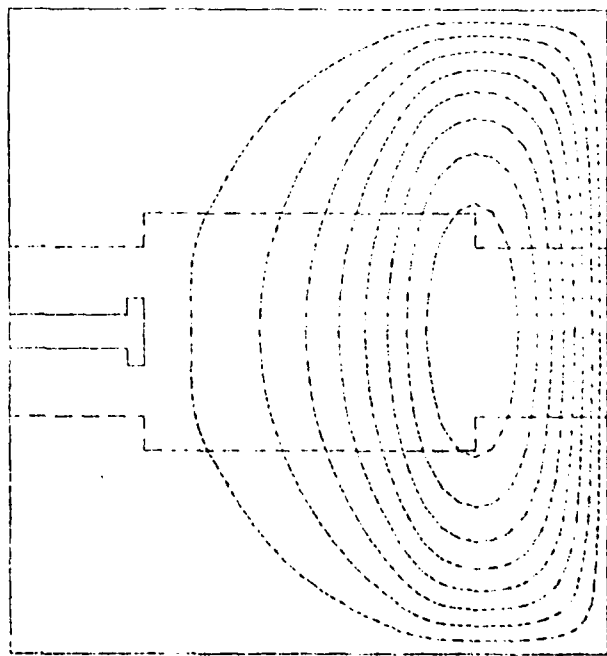
MINIMUM POTENTIAL	1.6V
MAXIMUM POTENTIAL	3.8V
CHARGE DENSITY IN FUEL	1.0E31
CHARGE DISTRIBUTION ON FOAM	1.0E22
FILLING LEVEL	1.0E22
CONTOUR SPACING	1.0V



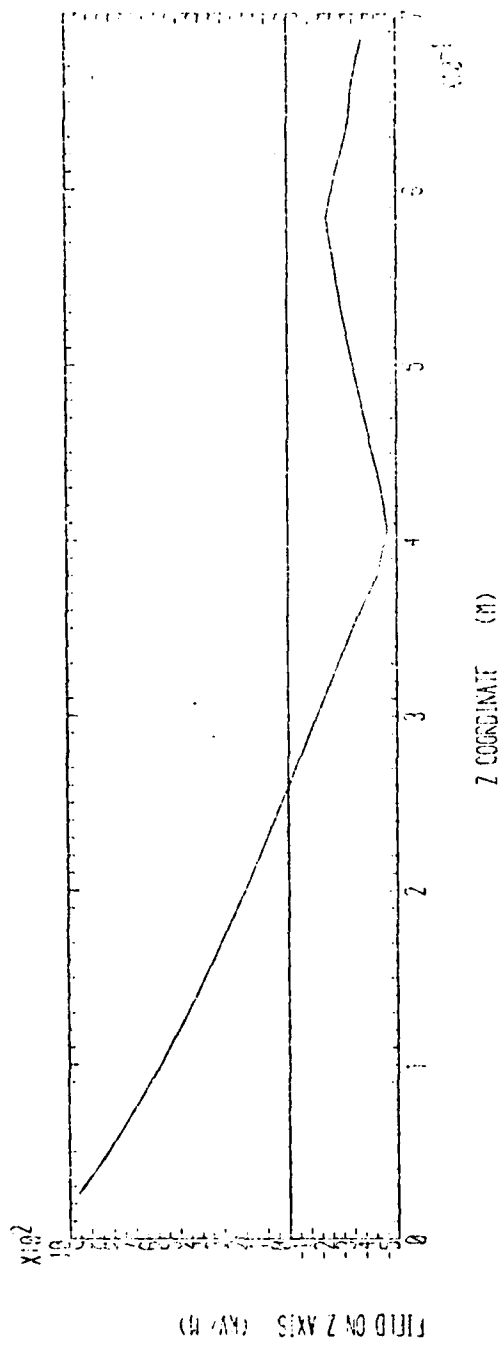
PLOT 32



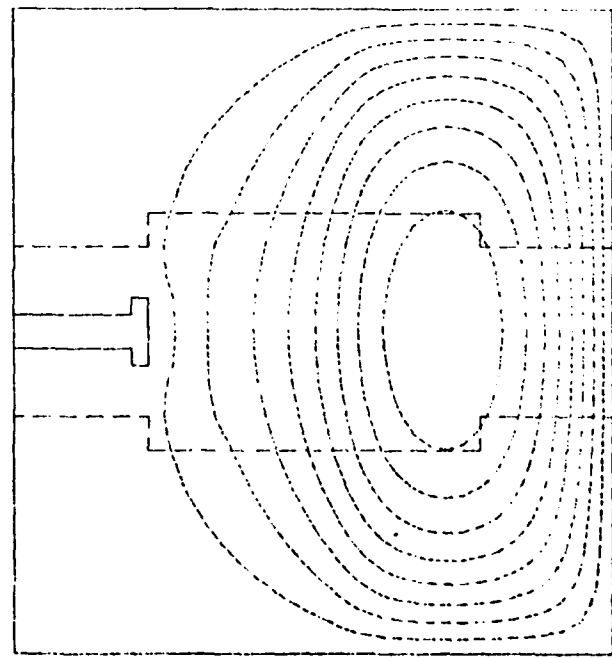
MINIMUM SIGHTING	1000' above sea level
MAXIMUM SIGHTING	1000' above sea level
CHASER DENSITY IN FIELD	1000' above sea level
CHASER DENSIFICATION IN FIELD	1000' above sea level
FALLING LEVEL	1000' above sea level
CONTINUOUS SPACING	1000' above sea level



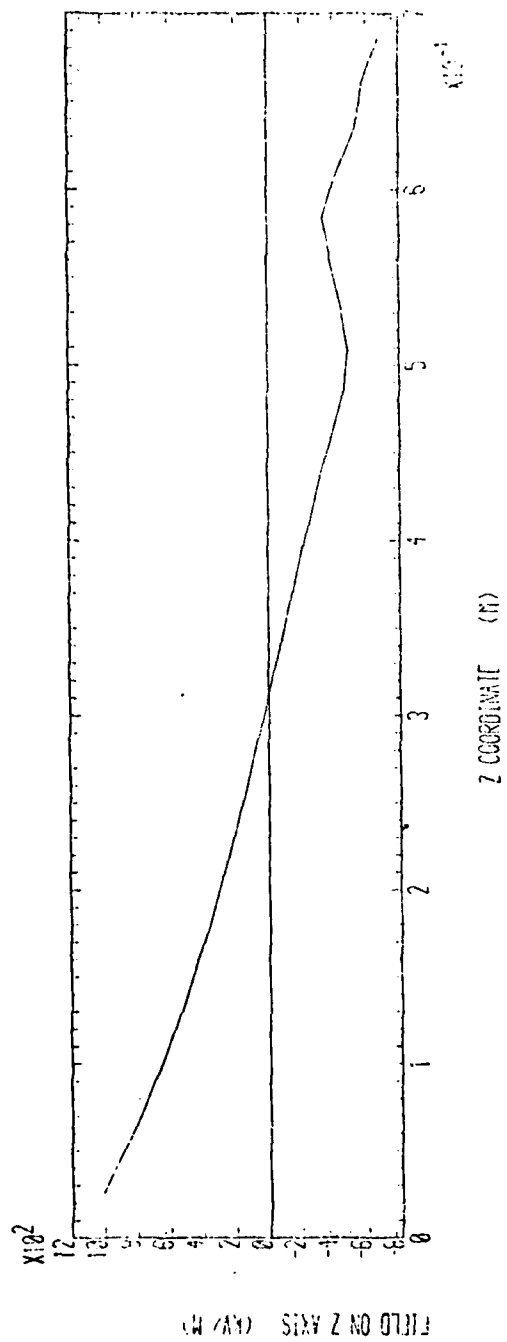
PLOT 33



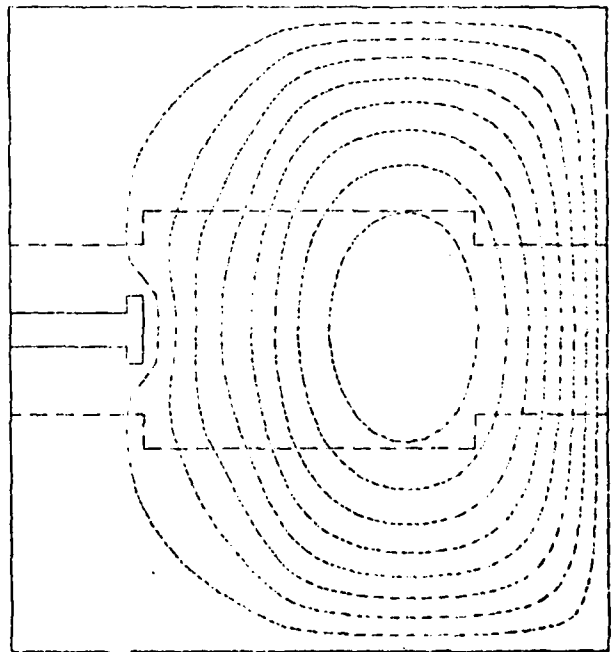
MINIMUM POTENTIAL	6KV	CONST.
MAXIMUM POTENTIAL	6KV	CONST.
CHARGE DENSITY IN FIGURE	2.25E-12	CONST.
CHARGE DISTRIBUTION ON FIGURE	1.0E-12	CONST.
FILLING LEVEL	0.52	CONST.
CONTOUR SPACING	0.5KV	CONST.



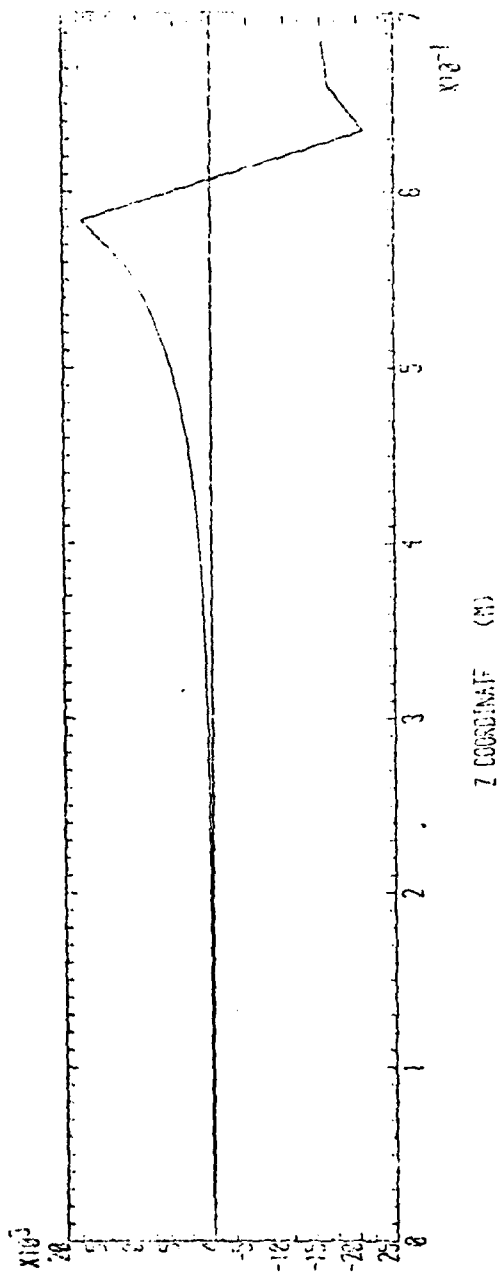
PLOT 34



MINIMUM POTENTIAL	10KV
MAXIMUM POTENTIAL	15KV
CHARGE DENSITY IN FOIL	1.0733
CHARGE DISTRIBUTION ON FOIL	1.0733
FILLING LEVEL	1.0733
CONTOUR SPACING	1.0733

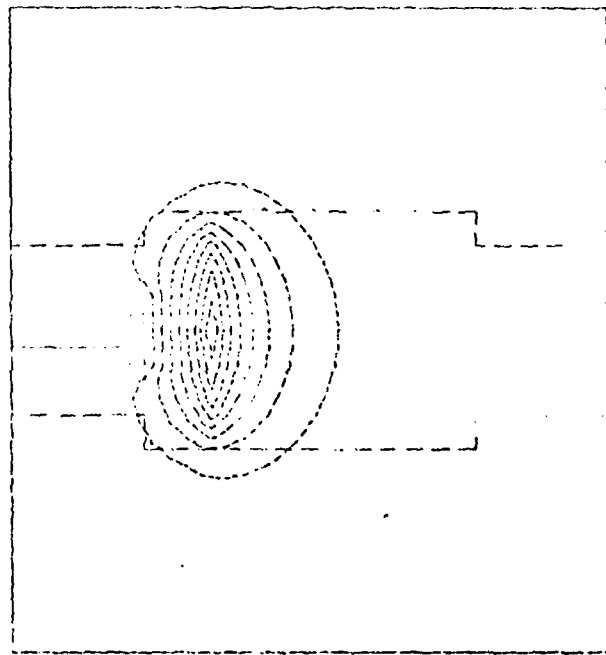


PLOT 35

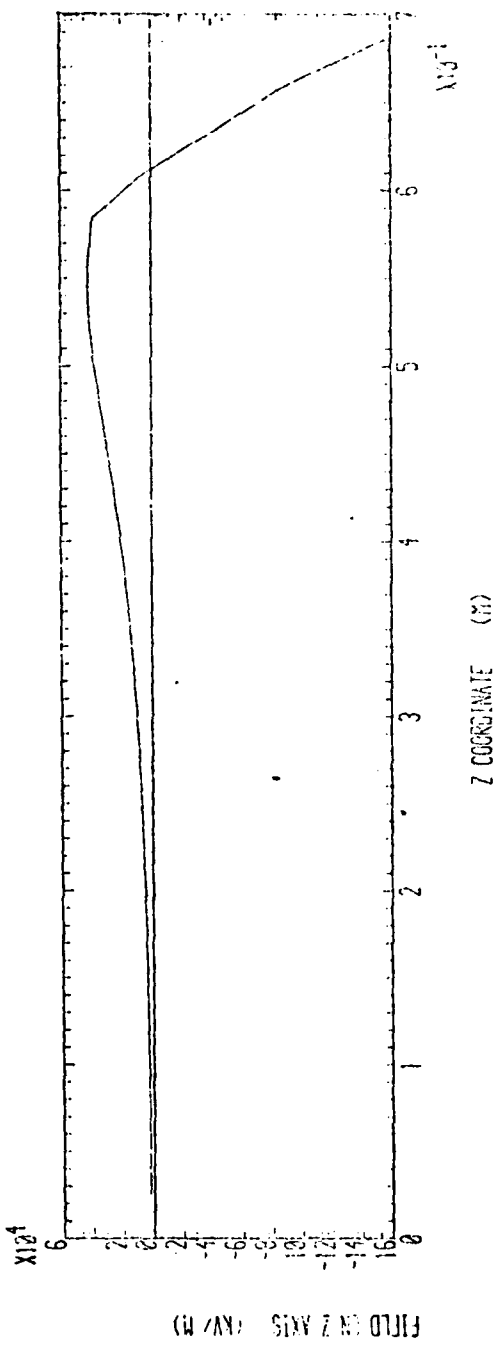


(2 AM) SIXTH TERM

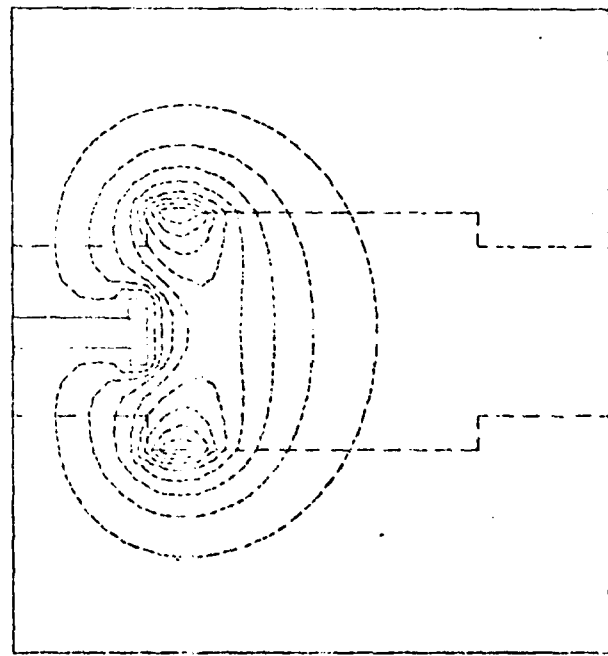
MINIMUM POTENTIAL	JK 3 .000E 0
MAXIMUM POTENTIAL	JKV .000E 0
CHARGE DENSITY IN FUEL	CM31 .000E 0
CHARGE DISTRIBUTION ON FCAN	COND1 .000E 0
FILLING LEVEL	LFL .000E 0
CONTAINER SPACING	SPAC1 .000E 0



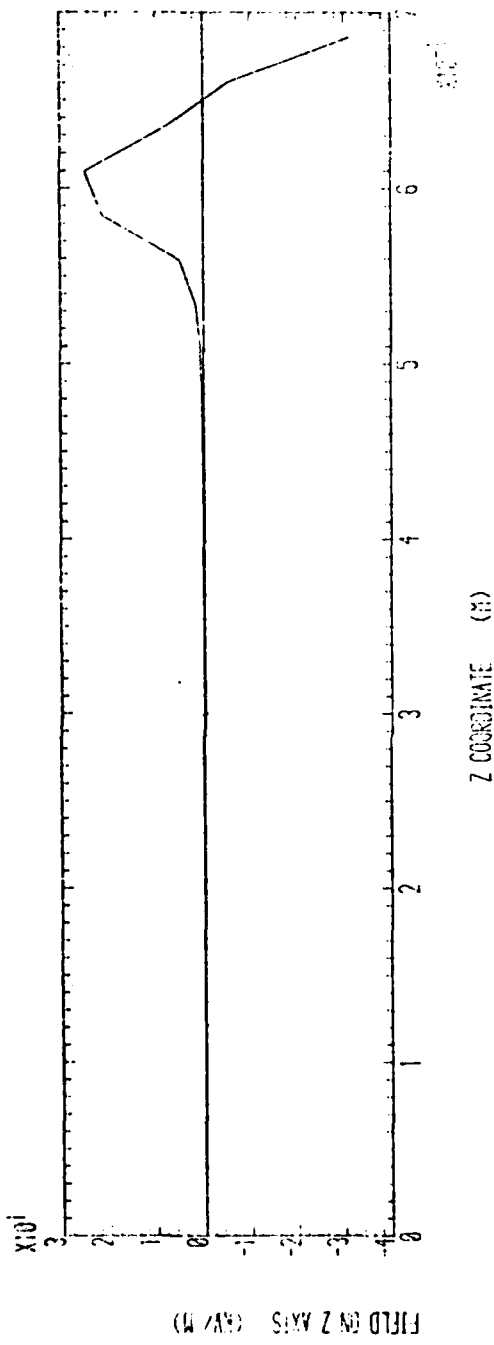
PLOT 36



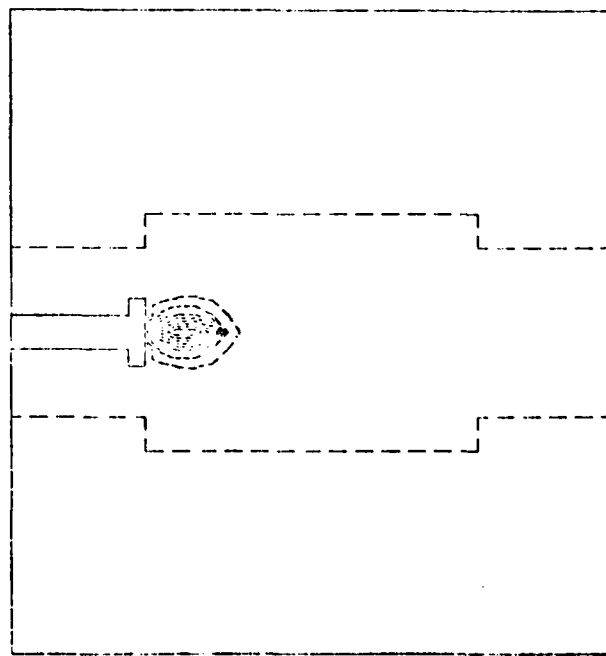
MINIMUM POTENTIAL	1KV .200E 0
MAXIMUM POTENTIAL	1KV .150E 0
CHARGE GEN IT IN FUEL	1KV .100E 0
CHARGE DISTRIBUTION ON FOAM	1KV .050E 0
FILLING LEVEL	.000 .400E 0
CONTOUR SPACING	.0KV .21667 E 0

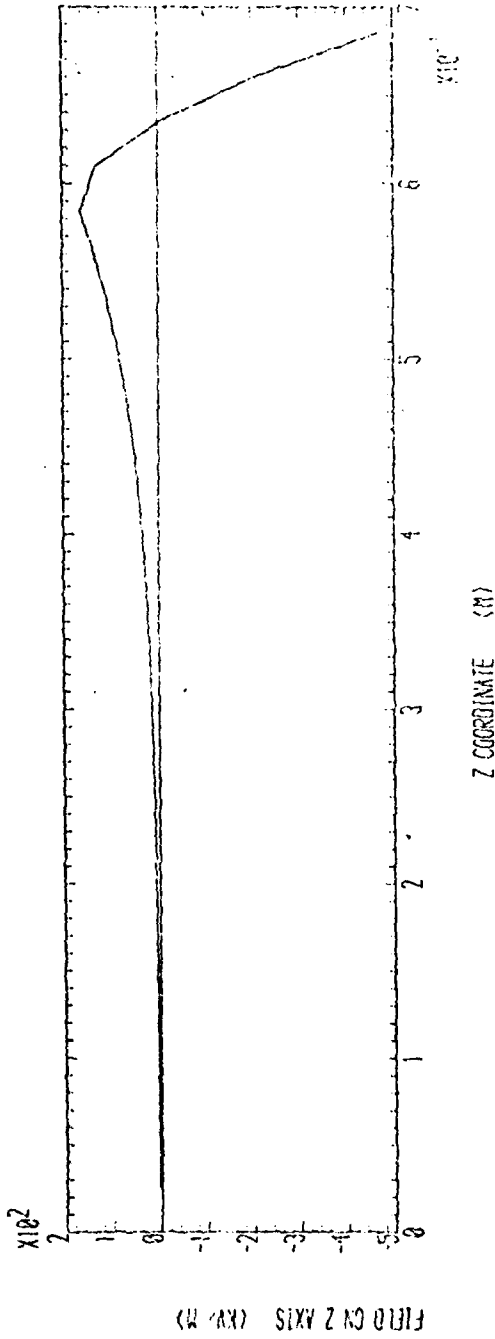


PLOT 37

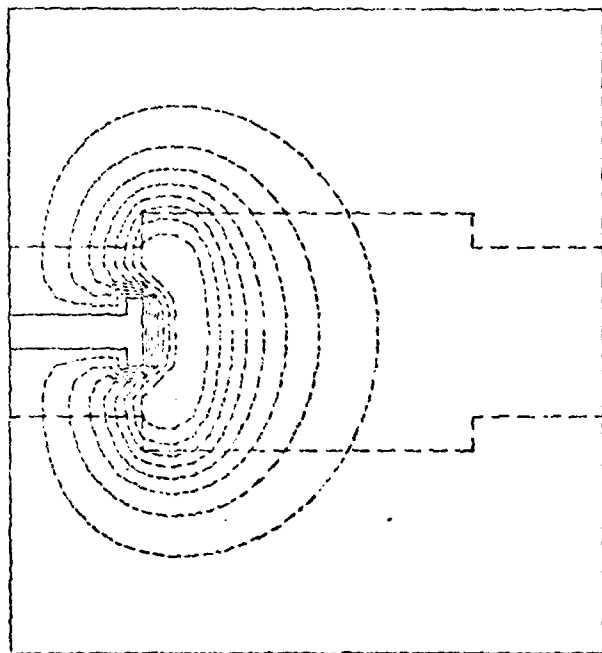


MINIMUM POTENTIAL	EKV1 .22626 0
MAXIMUM POTENTIAL	EKV1 .15915 0
CHARGE DENSITY IN FUEL	[CNS1] .33333 -3
CHARGE DISTRIBUTION ON FOAM	[CNS2] .33333 -3
FILLING LEVEL	LEB .22626 0
CONTOUR SPACING	EKV1 .17582 0





MINIMUM POTENTIAL (KV) .8333E 0
 MAXIMUM POTENTIAL (KV) .2666E 5
 CHARGE DENSITY IN FUEL (CM^-3) .6666E -3
 CHARGE DISTRIBUTION ON FOAM (CM^-2) .3333E 0
 FILLING LEVEL (M) .8333E 0
 FKV) .2587E 4
 CONTOUR SPACING

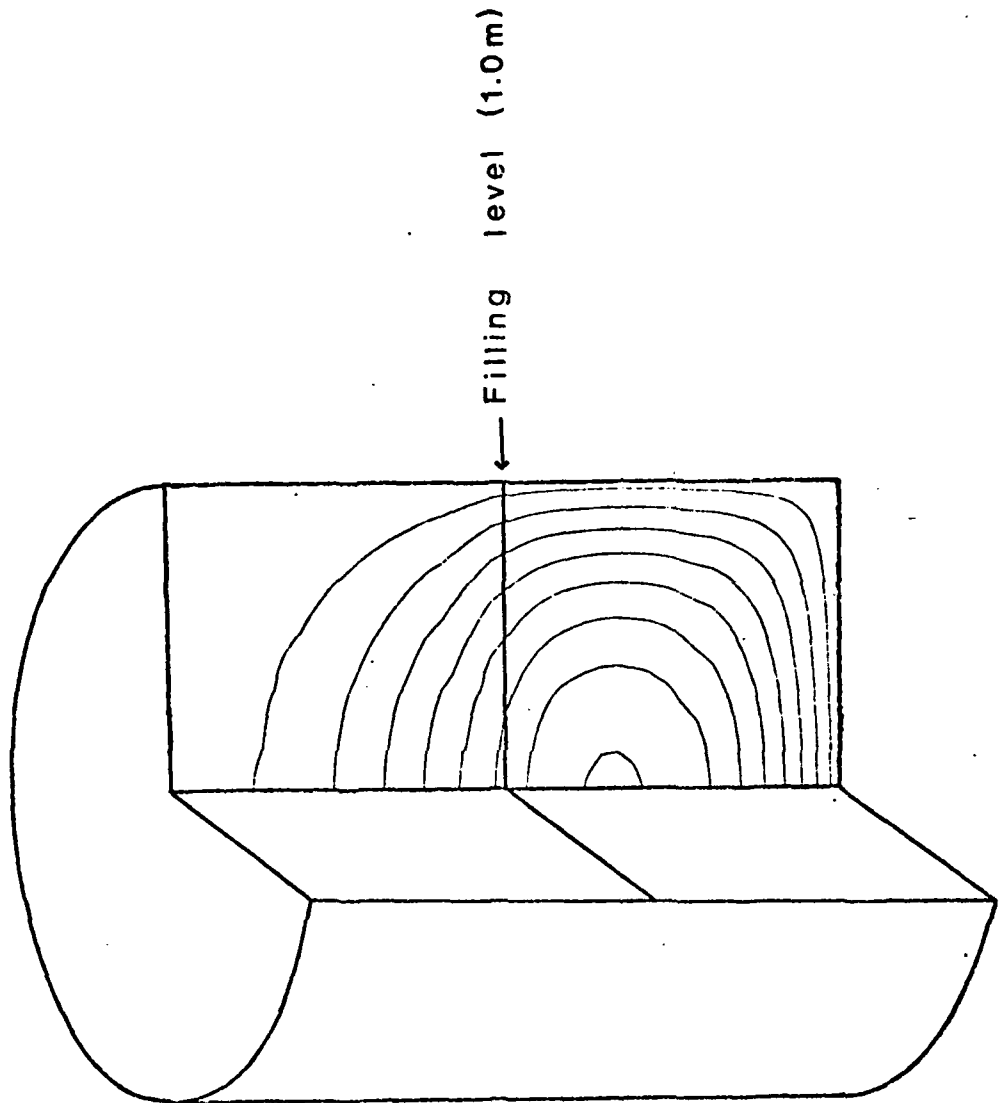


PLOT 39

APPENDIX A

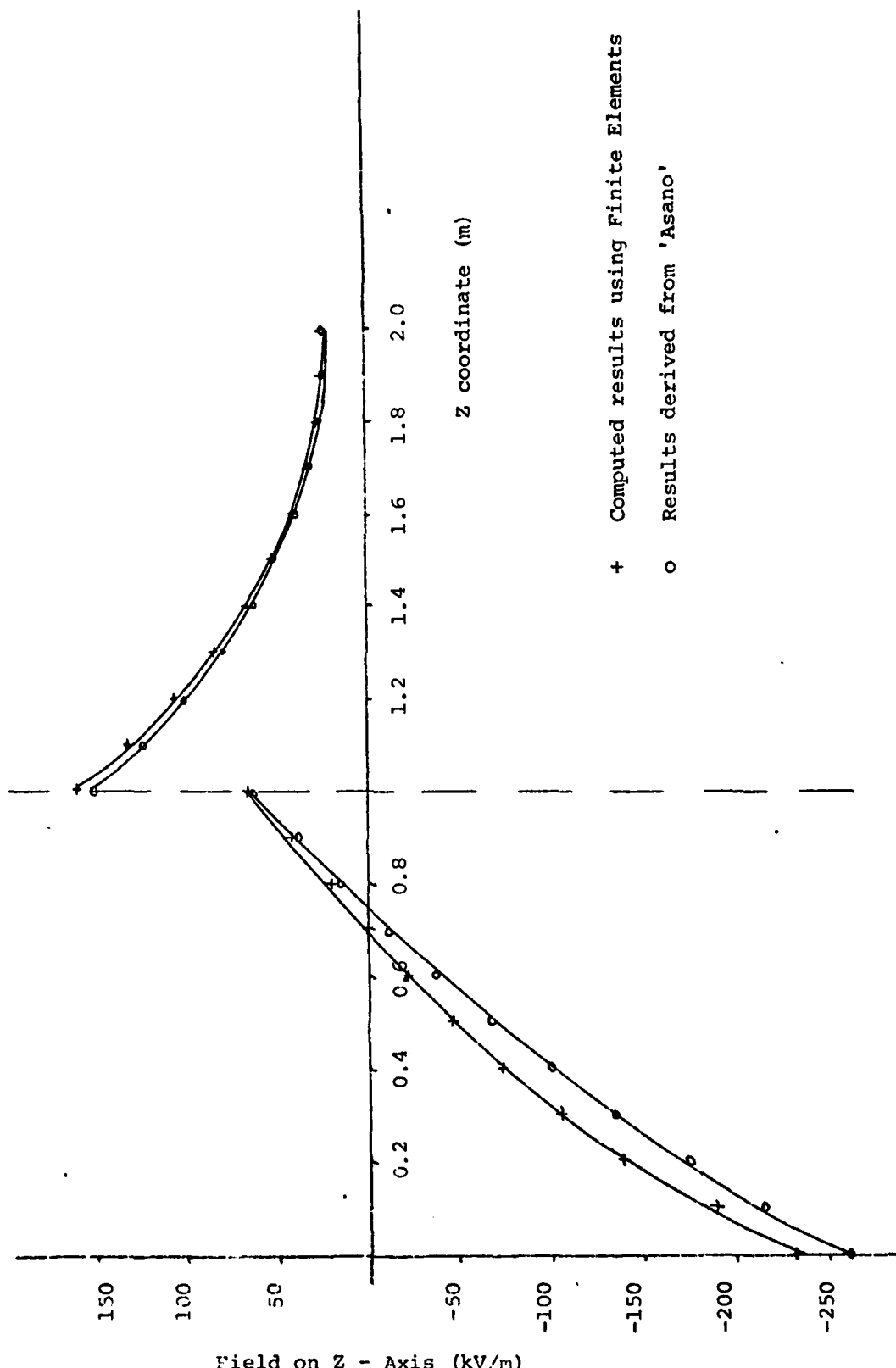
PROGRAM VALIDATION

The finite element program used in this study was written in FORTRAN. To test the accuracy of the program, it was checked against a problem for which an analytical solution has been found. Asano (Ref. 6) has provided an analytical solution for the potential in a cylindrical earthed metal tank half filled with charged liquid, assuming a uniform charge density. This problem was solved using the finite element program with a mesh of 760 nodes, and an equipotential map was drawn (Figure A1). The parameter chosen for comparison was the field along the cylinder axis. As can be seen from Figure A2, the finite element program produced results in good agreement with those of Asano.



Metal tank
Radius - 1.0 m
Height - 2.0 m

Fig. A1



Validation using 'Asano' results

Fig. A2

REFERENCES

1. E. Radgowski and R. Albrecht, "Investigation of electrostatic discharge in aircraft fuel tanks during refuelling", J. Aircraft, Vol. 16, No. 7, 1979 pp. 506-512.
2. S.J. Vellenga, "Estimating the electric field inside a rectangular tank with boundaries at zero potential", Appl. Sci. Res. 9, Section B.
3. J.A. Carruthers and K.J. Wigley, "The estimation of electrostatic potentials, fields and energies in a rectangular metal tank containing charged fuel", J. Inst. Petroleum, 48, 1962 pp. 181-189.
4. Electrostatic Test Summary, Aero Propulsion Laboratory, Wright-Patterson Air Force Base, 1980.
5. J.T. Leonard and W.A. Affens, "Electrostatic Charging of JP-4 fuel on polyurethane foams", NRL Report 8204, March 1978.
6. K. Asano, "Electrostatic potential and field in a cylindrical tank containing charged liquid", Proc. IEE, Vol. 124, No. 12, 1977 pp. 1277-1281.